2009

Heat transfer enhancement of spray cooling with nanofluids

Christian David Martinez
University of South Florida

Heat Transfer Enhancement of Spray Cooling with Nanofluids

by

Christian David Martinez

A thesis submitted in partial fulfillment
of the requirements for the degree of
Master of Science in Mechanical Engineering
Department of Mechanical Engineering
College of Engineering
University of South Florida

Major Professor: Frank Pyrtle III, Ph.D.
Muhammad M. Rahman, Ph.D.
Craig Lusk, Ph.D.

Date of Approval:
November 3, 2009

Keywords: nanoparticles, thermal management, critical heat flux, alumina, phase change

Dedication

I would like to dedicate this thesis to my parents because without them I would not have been able to accomplish this. I want to dedicate this to my dad because everyday he teaches me what is possible when you work hard and never look back, “ni para cojer empurso.” Also to my mom, because she always believed in me and knew that I could do it, even if sometimes I doubted it myself. Thank you for telling me to “keep going,” over and over again. I’m doing “good, good” now.

Acknowledgements

I would like to thank Dr. Pyrtle for his assistance in completing this thesis. Thank you for allowing me work with you under the *Research Experience for Undergraduates* program. Your heat transfer class was one of the main reasons I wanted to pursue a graduate degree. Thank you for all your help and knowledge.

I would also like to thank Dr. Lusk and Dr. Rahman for being part of my committee.

I would like to thank my lab partners John Shelton and Elliott Rice. Thank you John for helping me understand heat transfer better throughout the years and helping me assist students with their LabVIEW labs. Also, thank you for your assistance in the writing of this thesis. I would like to thank Elliott for having the same drive as I do to "always be the best." Thank you for studying with me for long hours and for your assistance during my thesis work.

I would like to thank Karen Mann for listening to me when I tried to explain what was going on with the spray cooling experiments and for helping me converting the thesis from Word documents into a single .pdf file.

Thank you all.

Table of Contents

List of Tables iii

List of Figures iv

Abstract vi

Chapter 1 – Introduction 1

Chapter 2 – Objective of Current Study 4

Chapter 3 – Literature Review 5

3.1 Nanofluids 5

3.1.1 Effects of pH on Nanofluids 6

3.2 Heat Transfer with Nanofluids 7

3.2.1 Transient Hot Wire Method Research 8

3.2.2 Pool Boiling Research 11

3.2.3 Impinging Jet Research 16

3.2.4 Spray Cooling Research 18

Chapter 4 – Experimental Set-up and Procedure 22

4.1 Nanofluid Preparation 22

4.2 Copper Block 24

4.3 Spray System 27

4.4 Spray Surface Preparation 28

4.5 Acquisition System 29

4.6 Surface Roughness Measurement 30

4.7 Experimental Procedure 31

Chapter Five – Results and Discussion 32

5.1 Uncertainty Analysis 32

5.2 Experimental Results 34

Chapter Six – Conclusion and Recommendations 53

6.1 Conclusion 53

6.2 Recommendations 54

References 55

List of Tables

Table 1: Summary Table 19

Table 2: Properties of Aluminum Oxide Nanoparticles 22

Table 3: pH Level of Selected Mass Concentrations 23

Table 4: Mass Flow Rates 28

Table 5: Critical Heat Flux for Water 37

Table 6: Critical Heat Flux for 1.0% wt. Alumina Nanofluids 40

Table 7: Critical Heat Flux for 0.5% wt. Alumina Nanofluid 43

Table 8: Critical Heat Flux for 0.1% wt. Alumina Nanofluid 45

List of Figures

Figure 1: pH Level vs. Mass Concentration of Alumina Nanofluids 23

Figure 2: Copper Block Design 25

Figure 3: Boundary Temperature Profile 26

Figure 4: Heat Flux Path through Block 26

Figure 5: Heat Flux Normal to Spray Surface 27

Figure 6: Schematic of Spray System 28

Figure 7: LabVIEW Front Panel 30

Figure 8: Spray Cooling Curve for Water at 40 Psi 35

Figure 9: Spray Cooling Curve for Water at 45 Psi 36

Figure 10: Spray Cooling Curve for Water at 50 Psi 36

Figure 11: Spray Cooling Curve Comparison of Water at Different Pressures 37

Figure 12: Spray Cooling Curve for 1.0% wt. AluminaNanofluid at 40 Psi 38

Figure 13: Spray Cooling Curve for 1.0% wt. Alumina Nanofluid at 45 Psi 39

Figure 14: Spray Cooling Curve for 1.0% wt. Alumina Nanofluid at 50 Psi 39

Figure 15: Spray Cooling Curve Comparison for 1.0% wt. Alumina Nanofluids at Different Pressures 40

Figure 16: Cooling Curve for 0.5% wt. Alumina Nanofluid at 40 Psi 41

Figure 17: Spray Cooling Curve for 0.5% wt. Alumina Nanofluid at 45 Psi 41

Figure 18: Spray Cooling Curve for 0.5% wt. Alumina Nanofluid at 50 Psi 42

Figure 19: Spray Cooling Curve Comparison for 0.5% wt. Alumina Nanofluids at Different Pressures 42
Figure 20: Spray Cooling Curve for 0.1% wt. Alumina Nanofluid at 40 Psi 43
Figure 21: Spray Cooling Curve for 0.1% wt. Alumina Nanofluid at 45 Psi 44
Figure 22: Spray Cooling Curve for 0.1% wt. Alumina Nanofluid at 50 Psi 44
Figure 23: Spray Cooling Curve Comparison for 0.1% wt. Alumina Nanofluid at Different Pressures 45
Figure 24: Spray Cooling Curve Comparison of Water vs. Nanofluids at 40 Psi 46
Figure 25: Spray Cooling Curve Comparison of Water vs. Nanofluids at 45 Psi 46
Figure 26: Spray Cooling Curve Comparison of Water vs. Nanofluids at 50 Psi 47
Figure 27: Surface Roughness before Spray Cooling 49
Figure 28: Surface Roughness after Spray Cooling with 0.5% wt. Alumina Nanofluid 50
Figure 29: Surface Roughness after Cleaning Procedure 50

Heat Transfer Enhancement of Spray Cooling with Nanofluids

Christian David Martinez

ABSTRACT

Spray cooling is a technique for achieving large heat fluxes at low surface temperatures by impinging a liquid in droplet form on a heated surface. Heat is removed by droplets spreading across the surface, thus removing heat by evaporation and by an increase in the convective heat transfer coefficient. The addition of nano-sized particles, like aluminum or copper, to water to create a nanofluid could further enhance the spray cooling process. Nanofluids have been shown to have better thermophysical properties when compared to water, like enhanced thermal conductivity. Although droplet size, velocity, impact angle and the roughness of the heated surface are all factors that determine the amount of heat that can be removed, the dominant driving mechanism for heat dissipation by spray cooling is difficult to determine.

In the current study, experiments were conducted to compare the enhancement to heat transfer caused by using alumina nanofluids during spray cooling instead of de-ionized water for the same nozzle pressure and distance from the heated surface. The fluids were sprayed on a heated copper surface at a constant distance of 21 mm. Three mass concentrations, 0.1%, 0.5%, and 1.0%, of alumina nanofluids were compared against water at three pressures, 40psi, 45psi, and 50psi. To ensure the suspension of the

aluminum oxide nanoparticles during the experiment, the pH level of the nanofluid was altered. The nanofluids showed an enhancement during the single-phase heat transfer and an increase in the critical heat flux (CHF). The spray cooling heat transfer curve shifted to the right for all concentrations investigated, indicating a delay in two-phase heat transfer. The surface roughness of the copper surface was measured before and after spray cooling as a possible cause for the delay.

Chapter 1 – Introduction

Gases or liquids impinging on a flat surface have been used to enhance the heating, cooling, or drying of a surface due in part to the increase in convection heat transfer coefficient. The delivery of the gas or liquid to the surface has been achieved by the use of a single nozzle or an array of nozzles usually oriented normal to the target surface. Impinging jets have been used in many applications including the annealing of metals and the cooling of gas turbine blades. One particularly important application of impinging jets is the spray cooling of high performance electronic devices (Incropera, DeWitt, Bergman, and Lavine 402). The need for these electronic devices to be smaller and faster requires the removal of large heat fluxes to keep the product working and extend its life cycle. Currently, many electronic devices use a heat sink and fan combination to remove heat because of their simplicity and low cost. The heat sink conducts heat from the heated surface efficiently because of its high thermal conductivity and dissipates the heat through its fins to the surroundings via forced convection using a fan when is usually mounted on top of the heat sink. Another popular way to remove heat is by the use of heat pipes. Heat pipes most commonly use the evaporation of water or some kind of coolant to remove heat from a heated surface. The hot end of the heat pipe vaporizes the working fluid increasing the vapor pressure at that end providing the driving force needed to move the vapor to the cooler condensing end and providing the hot end with the lower temperature working fluid once again.

Both the heat sink and the heat pipe, though they are widely used, have their limitations. To be effective at removing and the spreading the heat, the heat sink needs to be a number of times larger than the heated surface, usually a computer processing unit or CPU, leading to a size constraint of the electronic device. Also, parts of the heat sink, like the pins, that are father away from the heat source are, by nature, cooler which reduces the rate of heat transfer. Heat pipes suffer from different limitations. Since most heat pipes depend on pressure differences to remove heat, the interaction between the liquid and vapor phases can cause the heat transfer rate to deteriorate because of pressure losses caused by entrainment. To remove large amounts of heat with heat pipes requires longer distances to avoid vaporizing all the liquid in the heat pipe rendering it useless. One way to remove large amounts of heat from CPU's and other similarly heated surfaces without the need for long distances or large pieces of metals and fans is with spray cooling.

Spray cooling typically involves the phase change heat transfer of a liquid to a vapor by impingement on a flat heated surface. The most common fluid used is water because of its well known thermal properties, abundance, cost effectiveness, easiness to store and it's harmlessness to the environment. Typically, the water is delivered to the surface in a mist through the use of a round or rectangular nozzle. The enhancement for removing large quantities of heat comes from the increased value of the convection heat transfer coefficient. The convection heat-transfer coefficient during spray cooling varies not only with the temperature between the surface and the fluid but also with the spray's characteristics. The spray's characteristics include but are not limited to: temperature and thermal conductivity of the water, droplet size, velocity and angle. If the thermal

properties of the water were to be enhanced then, theoretically, that should lead to an enhancement of convection heat transfer coefficient and increase the heat that can be removed from the surface.

One way to change the thermal physical properties of water is by the addition of nano-size particles to create a nanofluid [Choi]. Research on nanofluids has shown an increase in the thermal conductivity over the base fluid alone [Choi]. The increase in the thermal conductivity of water has the potential to enhance the heat flux removed from a heated surface during spray cooling by increasing the convective heat transfer coefficient. There are other properties that can affect the effectiveness of spray cooling using nanofluids, like the surface roughness of the heated surface, that also need to be investigated.

Chapter 2 – Objectives of Current Study

The objective of the current study is to determine the effectiveness of alumina nanofluids for dissipating heat from a heated copper surface using a lateral spray cooling experiment. The data collected is compared to de-ionized water at the same nozzle pressure and distance from the surface. Different mass concentrations of alumina nanofluids at different pressures will be compared to attempt to establish an optimum combination of concentration and pressure. Other parameters can have an effect on the effectiveness of spray cooling, such as the surface roughness of the impinged surface. Therefore, the surface roughness of the copper surface is recorded before and after spray cooling with the alumina nanofluid to investigate the effects of the nanoparticles on the copper surface.

Chapter 3 - Literature Review

3.1 Nanofluids

There are many different types of nanofluids that can be made by using different nanoparticles and base fluid combinations. Some of the most common nanoparticles used are Alumina Oxide (Al_2O_3), Copper II Oxide (CuO), Zinc Oxide (ZrO_2), and Silica Oxide (SiO_2). The most common base fluids used for nanofluids are de-ionized water and ethanol.

All nanofluids follow a basic preparation technique. Once the desired weight or volume fraction has been determined, the nanoparticles are added into the base fluid and mixed. Mixing is usually done by ultrasonication to avoid settling of the particles. The amount of time spent mixing the nanofluids depends on the many factors such as the ratio of base to nanoparticles, how long the experiment will last, and the weight or volume fraction used.

The results of the first research into nanofluids conducted by Choi *et al.* (1995) showed that these new nanofluids had tremendous heat transfer applications because of their improved heat transfer properties. A lot of research has gone into finding exactly why nanoparticles have such enhancement to heat transfer properties of the fluid but no definitive answers have been found. Jang *et al.* (2004) and Chon *et al.* (2005) have theorized that microconvection induced by Brownian motion of the nanoparticles is one

of the driving mechanisms behind the thermal enhancements of nanofluids. The random motion of the nanoparticles would create a source of fluid convection that would increase the thermal properties of the base fluid. Most researchers agree that nanofluids have been shown experimentally to have better heat transfer properties than the base fluid alone. Another advantage of utilizing nanofluids is that at the nano-scale the particles are small enough to stay in suspension, under the right conditions they can stay in suspension indefinitely, effectively eliminating sedimentation, clumping, and clogging.

3.1.1 Effects of pH on Nanofluids

One of the most common challenges in using nanofluids is maintaining the suspension of the nanoparticles within the fluid. Anoop *et al.* (2009) was able to accomplish suspension of aluminum oxide particles for several weeks by altering the pH value of the nanofluid. By keeping the nanofluid away from the iso-electric point (IEP), the point where there is zero net charge between the particles and the bulk fluid, the particles were kept in suspension by the electrostatic repulsive forces between them. The pH values of 1 wt%, 2 wt%, 4 wt% and 6 wt% were found to be 6.5, 6, 5.5, and 5 respectively.

The dispersion behavior and thermal conductivity of Al_2O_3 – water nanofluids under different pH levels were investigated by Zhu *et al.* (2009). For all the experiments a 0.1 wt% alumina nanofluid concentration was used. To control the pH level of the nanofluid Zhu *et al.* used analytical grade hydrochloric acid (HCl) and sodium hydroxide (NaOH). To aid in the initial dispersion of the nanoparticles an ionic surfactant, sodium dodecylbenzenesulfonate (SDBS), was added to the mixture and then mixed in an

ultrasonicator. Zhu *et al.* found that for an alumina nanofluid containing SDBS as a surfactant, the optimum pH value is 8.0. This is the point with the greatest value of zeta potential and therefore the particles have the highest electrostatic repulsive forces, which keep the particles in suspension. The thermal conductivity of the alumina nanofluid was measured by the transient plane source (TPS) method. Through the investigation it was found that there is an increase in thermal conductivity for pH values from 3.0 to 8.0-9.0. Zhu *et al.* suggest that as the pH level of the nanofluid increases farther away from the point of zero change (PZC), the point where there are no repulsive forces between the Al_2O_3 nanoparticles, therefore they coagulate. As a result, the hydration forces are greater between the particles. The increase in hydration forces causes an enhancement in the mobility of the nanoparticles. The mobility of the nanoparticles creates microscopic motions that cause microconvection which enhances the heat transfer process.

3.2 Heat Transfer Research with Nanofluids

It's been shown that nanofluids in general have better heat transfer properties than the base fluid alone, specifically better thermal conductivity and heat transfer coefficient. These heat transfer properties theoretically should make nanofluids ideal for phase change heat transfer processes. These enhancements have been researched using experiments such as the transient hot wire method, pool boiling, impinging jet and nanofluid tube flow.

3.2.1 Transient Hot Wire Method Research

The transient hot wire method (THW) is a transient dynamic technique where the temperature rise of a sample is measured at a defined distance from a heat source. The hot wire is assumed to have a uniform heat output along its length and the thermal conductivity of the sample can be calculated from the temperature change of the sample over a known time interval.

The thermal conductivity of different concentrations of water-copper and transport oil-copper nanofluids were investigated by Xuan *et al.* (2000) by the use of the transient hot wire method. To calculate the thermal conductivity of the nanofluids, Xuan *et al.* used the fundamental equation of the transient hot wire method, give by:

$$\Delta T(r,t) = \frac{q}{4\pi k} \ln \frac{4at}{r^2 C},$$

where k is the thermal conductivity of the sample, a is the thermal diffusivity, and C is given by:

$$C = e^g,$$

where g (g = 0.5772157) is Euler's constant. The results show that one of the factors affecting the thermal conductivity of nanofluids is the nanoparticle volume fraction. An increase in volume fraction results in an increase in the thermal conductivity of both the water-copper and the transformer oil-copper nanofluids. For example, the water-copper nanofluid saw an improvement in the thermal conductivity ratio of nanofluid to water from 1.24 to 1.78 with an increase of volume fraction of 2.5% to 7.5%. Hwang *et al.* (2006) also investigated the effects of nanoparticle concentration on the thermal conductivity of nanofluids using the THW method. The investigation was conducted

with multiwalled carbon nanotubes (MWCNT) in water, copper monoxide (CuO) in water, silicon dioxide (SiO_2) in water, and CuO in ethynele glycol. The results of the investigation were similar to Xuan *et al.*, where an increase in the thermal conductivity of the nanofluids was obtained with an increase in the volume fraction concentration of the nanoparticles. Hwang *et al.* also reported that the thermal conductivity of nanofluids were also dependent on the thermal conductivity of the nanoparticles and the base fluid. For instance, for the same volume fraction concentration of 1% the CuO-water nanofluid saw an increase in the thermal conductivity of approximately 5% when compared to an improvement of approximately only 3% for SiO_2-water nanofluids. One possible factor for the difference in improvement is the thermal conductivity of the nanoparticles, 76.5 W/mK for CuO compared to only 1.38 W/mK for SiO_2. Different enhancements in thermal conductivity where also acquired for nanofluids with the same nanoparticles but different base fluids. The enhancement to thermal conductivity for CuO-ethynele glycol nanofluids was higher than that for CuO-water nanofluids for the same volume fraction concentration. The results show that the base fluid with the lowest thermal conductivity will benefit more from the addition of nanoparticles, in this case the ethynele glycol with a thermal conductivity of 0.252 W/mK compared to that of water with 0.613 W/mK. Zhang *et al.* (2006) used a method based on the THW method called the short hot wire (SHW) method to conduct experiments with different nanoparticle and base fluid combinations. Different concentrations of nanoparticles and the temperature of the nanofluid are investigated for their effects on the thermal conductivity of the nanofluid. In the study gold (Au)-toluene nanofluid at a volume fraction of 0.003%, Al_2O_3-water nanofluids with mass concentrations of 0%, 10%, 20% and 40%, and carbon nanofiber

(CNF)-water nanofluids with a volume concentration range of 0 to 1% are investigated. Zhang *et al.* also recorded increases in thermal conductivity of all nanofluids investigated corresponding to increases in the concentration of the nanoparticles and the temperature of the nanofluid. The slope of the dependence of the thermal conductivity on temperature for nanofluids was compared to pure water and it was found that the slopes were the same. The results indicate that the temperature dependence on the thermal conductivity and thermal diffusivity of the nanoparticles do not have an affect on the thermal conductivity and thermal diffusivity of the nanofluid for the given concentrations. Xie *et al.* (2002) also used the THW to study the thermal conductivity of nanofluids by looking at different volume fractions of Al_2O_3 particles suspended in de-ionized water, ethanol, and pump oil, different specific surface areas, and by looking at the different pH values of the nanofluid. Xie *et al.* found that for all the base fluids the thermal conductivity increases with increasing volume fraction but with different slopes, corresponding to different pH values. The results show that with an increase in pH level the enhanced thermal conductivity ratio decreases. When the difference between the pH value of the suspension and the isoelectric point increases, the hydration forces among the particles start to increase which leads to an enhancement of the mobility of the nanoparticles in the fluid. This enhancement in the mobility of nanoparticles causes microconvection that enhances the heat transfer process. The results show that there is an optimum specific surface area of the nanoparticles that enhance thermal conductivity. The thermal conductivity increases with increasing specific surface area at first but then begins to decrease. The optimum specific surface area for this study is found to be $25\,m^2 g^{-1}$. One of the factors for this change in thermal conductivity is that as the particle size of the

nanoparticle decreases, the specific surface area increases proportionally. Since heat transfer in nanofluids occur at the particle-fluid interface, a reduction in particle size can result in a large interfacial area. Murshed *et al.* (2005) prepared nanofluids by dispersing titanium oxide (TiO_2) nanoparticles in rod and spherical shapes in de-ionized water to conduct THW experiments. The results show that the thermal conductivity increases with increasing nanoparticle volume concentration. The shape of the nanoparticles also affects the thermal conductivity of the nanofluid. The rod shaped TiO_2 nanoparticles showed an enhancement of 33% in thermal conductivity when compared to the base fluid alone at a volume concentration of 5%. In comparison, the spherical shaped nanoparticles showed an enhancement of 30% at the same volume concentration.

3.2.2 Pool Boiling Research

Pool boiling is the process in which vapor is created at the liquid-surface interface by a surface heated above the saturation temperature of the bulk fluid. The motion of the vapor and the surrounding fluid near the heated surface is due to buoyancy forces. As vapor escapes the surface, liquid comes in to fill the void and this process removes heat from the heated surface.

Bang *et al.* (2005) investigated the boiling heat transfer characteristics in different volume concentrations of alumina nanofluids and compared the results to pure water. Both vertical and horizontal heated surfaces were considered for the experiment. The research shows that the addition of alumina nanoparticles causes the boiling curve to shift to the right, which means that there are decreases in the pool nucleate boiling heat transfer for all concentrations. Also, it was observed that the nucleate boiling regime was

delayed due to an extended natural convection stage which is inconsistent with the increase in thermal conductivity of nanofluids. On the other hand, the critical heat flux (CHF) was increased by 32% and 13% for horizontal and vertical heaters respectively. Bang *et al.* suggested that the fouling of the heated surface by the alumina nanoparticles caused a decrease in the nucleation site density. Large vapor blankets close to the surface are generated with the decrease in nucleation sites which allows more water to be supplied to the heated surface. You *et al.* (2003) conducted pool boiling experiments of Al_2O_3 water nanofluids at a pressure of 2.89 psia which gives a saturation temperature of 60 ˚C using a 1 x 1 cm^2 polished copper surface. The nanoparticle mass concentrations ranged from 0 g/l to 0.05 g/l and their results were compared to de-ionized water. The results show an increase in the CHF with an increase of mass concentration. A remarkable increase of 200% enhancement was shown with a 0.05 g/l mass concentration. Another result of the study shows that the average size of the bubbles increased and the frequency decreased with the use of nanofluids. You *et al.* concludes that the increase in the CHF is not related to the increase in thermal conductivity by the addition of nanoparticles. Das *et al.* (2003) also investigated the boiling heat transfer characteristics of 1%, 2%, and 4% concentration alumina nanofluids with similar results to those obtained by Bang *et al.* The boiling curve again showed a shift to the right with increasing concentration of nanoparticles. Das *et al.* considered the surface roughness of the heaters as one of the factors for the degrading of the heat transfer performance. Surface roughness measurements of the heated copper surface showed that after pool boiling experiments with nanofluids, the surface of the heater was smoother than before the experiment. The results suggest that the alumina nanoparticles are being trapped on

the surface, since the size of the particles were one to two orders of magnitude smaller than the roughness. The trapped particles form a layer on the heated surface hindering fluid flow and heat transfer, which may explain the degrading of boiling heat transfer performance when compared to water. Das *et al.* again investigated 1%, 2%, and 4% concentration of alumina nanofluids on pool boiling but on narrow horizontal tubes. The tubes were 4 and 6.5 mm in diameter. Once again, a deterioration of the pool boiling heat transfer curve resulted with increasing nanoparticle concentration. The deterioration was less significant for the narrow tubes than tubes of a larger diameter (20 mm). Less deterioration in the narrow tubes was believed to be due to the change in bubble diameter and sliding bubble mechanism when compared to the larger diameter tubes. Das *et al.* concluded that there are two conflicting phenomena occurring with pool boiling heat transfer with nanofluids. The addition of nanoparticles increases the viscosity of the base fluid which increases the heat transfer of the base fluid but it is overshadowed by the decrease in the nucleation site density due to nanoparticles impinging on the surface. Zhou *et al.* (2004) conducted pool boiling experiments with different concentrations of Cu-acetone nanofluids and with acoustic cavitations. Cavitations are the sudden formation and collapse of low-pressure bubbles due to mechanical forces. In this experiment ultrasound was created by an ultrasonic vibrator. Acoustic cavitations enhance heat transfer by utilizing the energy released by the collapsing low-pressure bubbles. An increase in single-phase heat transfer was found with increasing concentration. Though a degrading of pool boiling heat transfer was found, Zhou *et al.* noted that when the concentration increased from 0.133 g/l to 0.267 g/l no further degrading was noticed. This result is substantially different than the work done by Das *et*

al. who found that heat transfer reduced with increasing nanoparticle concentration. The thermophysical properties of the nanoparticles are though to be a reason for this discrepancy. At all the nanoparticle concentrations investigated the acoustic cavitations were shown to enhance heat transfer. As the distance between the sound source and the heated copper surface increased from 20 mm to 40 mm, only a slight decrease in pool boiling heat transfer was noticed. Different volume fractions of a different nanofluid, titanium dioxide and the refrigerant HCFC 141b, was investigated by pool boiling by Trisaksri *et al.* (2009). The investigation used 0.01, 0.03, and 0.05 vol% of TiO_2 and a cylindrical copper tube as the boiling surface. The first results from the experiment reveal that for the 0.01 vol% concentration the boiling heat transfer is the same as the base fluid alone. This shows that adding very small amounts of nanoparticles to the base fluid had no effect on boiling heat transfer. At 0.03 and 0.05 vol% concentration the boiling curve is shifted to the right indicating a deterioration of boiling heat transfer, which supports the results by Bang *et al*. One explanation for the shift of the boiling curve is the range of the excess temperature in the natural convection regime of the nanofluid is larger than that for the base fluid alone; this causes a delay of nucleate boiling and a rise in the surface temperature. Trisaksri *et al.* also looked at the effects of pressure on the heat transfer coefficient. At lower concentrations, 0.01 and 0.03 vol%, the effects of pressure on heat transfer coefficient are negligible. However, at 0.05 vol% there is a rise in the heat transfer coefficient at high heat fluxes. The rise in heat transfer coefficient is lower than the rise seen for the base fluid alone. Wen *et al.* (2008) conducted a pool boiling experiment using different particle concentrations in alumina nanofluids with different results. The results show that there is an enhancement of both

boiling heat transfer coefficient and thermal conductivity when compared to the base fluid. The improvement increases with increasing nanoparticle concentration and is more significant at higher heat fluxes. Enhancement of up to 40% in heat transfer coefficient was achieved with a concentration of 1.25 wt%. With an increase of 10% with a concentration of 1.6%, the enhancement to the thermal conductivity was not as significant as for the heat transfer coefficient. Wen *et al.* suggests nanoparticle migration as one of the reasons for the enhancement in heat transfer coefficient and thermal conductivity and the depositing of nanoparticles on the heated surface, which introduces a thermal resistance, as one of the reasons for the deterioration that has been seen in other studies. Vassallo *et al.* (2004) pool boiling experiment was done using silica oxide nanofluids with different particle sizes. In this experiment there was no decrease in the heat transfer coefficient, but no improvement was found either. The boiling curve for both particle sizes, 15nm and 50nm, follow the pure water boiling curve through the nucleate boiling regime. Again, an increase in the CHF was found. Coursey *et al.* (2008) researched an improvement in surface wettability as the possible mechanism for the increase in CHF. Wetting is the ability of a fluid to remain in contact with a solid surface. It was found that nanoparticles had a positive effect when there was a large contact angle between the fluid and the solid surface, which means that the surface is difficult to wet or the base fluid is less wetting. For fluids that are naturally more wettable, for example ethanol, the addition of nanoparticles had little to no effect on wetting. Water had increase in wetting with the addition of nanoparticles because it is a naturally less wettable fluid. The increase in wetting was found to be one of the driving mechanisms to improving the CHF. The conflicting results in heat transfer and thermal

conductivity by the addition of nanoparticles to a base fluid shows that the further research is needed in this field.

3.2.3 Impinging Jet Research

Impinging jet research is another way to study the effects that nanoparticles have on the heat transfer coefficients of the base fluids. A nozzle is used to spray a jet of fluid onto a heated surface to enhance the heat transfer coefficients for convective heating, cooling, or drying.

Nguyen *et al.* (2009) used a nozzle with a diameter of 3mm to spray a 36nm alumina nanofluid onto a confined and submerged heated aluminum surface. Nguyen *et al.* tested different concentrations of nanoparticles, 0%, 2.8%, and 6%, with different flow rates and nozzle-to-surface distances. The research shows that in some cases the addition of nanoparticles increases the heat transfer coefficient of the base fluid. With a mass flow rate of 0.15 kg/s and a nozzle-to-surface distance of 2mm, the pure water has the highest heat transfer coefficient followed by 2.8% concentration and finally 6% concentration. With the same mass flow rate but with a distance of 5mm, the 2.8% concentration of nanoparticles was found to give the highest heat transfer coefficient followed by water then 6% concentration. At 10mm nozzle-to-surface distance, water and 2.8% concentration have almost the same heat transfer coefficient, while the 6% concentration came in at third place. The study shows that there is an optimum nanoparticle concentration, flow rate, and nozzle-to-surface distance that will give the best results. Also, concentrations greater than 6% should be avoided for impinging jet cooling. Liu *et al.* (2007) conducted impinging jet research using CuO nanoparticles

suspended in water. The effects of nanoparticle concentration and the flow conditions were investigated and compared to the base fluid. The impingement took place in a 20mm diameter heated copper surface with a 4mm diameter nozzle and the mass concentrations of CuO nanoparticles changed from 0.1 to 2 wt%. The results of the study show that the jet boiling curves for all nanoparticle concentrations are shifted to the right, indicating a deterioration of boiling heat transfer when compared to the base fluid. For the range tested, the different nanoparticle concentrations had little effect on the boiling heat transfer. At higher jet velocities, as expected, the boiling heat transfer increases. The critical heat flux (CHF) of the nanofluids increased, up to 25% compared to water, with increasing concentrations at a low range. At 1 wt% no more increase in CHF was noticed. Liu *et al.* conducted surface roughness measurements before and after impinging jet with the base fluid and the nanofluid. After the water jet impingement experiments were conducted the surface had become slightly oxidized. The existence of a thin sorption layer was present after the nanofluid impingement test. The sorption layer made the copper heater surface smoother, thus decreasing the number of nucleation sites. The sorption layer could explain the decrease in boiling heat transfer and the increase in CHF. The decrease in nucleation sites and the increase in thermal resistance caused by the sorption layer could be a reason for the decrease in boiling heat transfer. The existence of the sorption layer also enhances the trapping of liquid in the porous layer and prevents vapor blankets from forming leading to an increase in CHF.

3.2.4 Spray Cooling Research

Another method that utilizes the impingement of a working fluid onto a heated surface is spray cooling. During spray cooling the pressure difference between the nozzle and the environment is sufficient to create droplets of the working fluid and those droplets impinge the surface to remove heat.

Shen (2009) investigated the hydrodynamic characteristics of droplets impinging on a polished and a nano-structured heated surface. The results of a single-wall-carbon-nanotube nanofluid were compared to water. The addition of nanoparticles resulted in larger spreading velocities, larger spreading diameters, and an increase in early stage dynamic contact angle. It was found that the evaporation time was reduced by 37% with the use of nanofluids on the polished surface. The combination of the nanofluid and the nano-structured surface yielded reduced evaporation times of 20%. The reduction of the evaporation time indicates an enhancement to heat transfer for evaporative cooling. Coursey (2007) has added high aspect ratio microchannels to the copper sprayed surface resulting in very high enhancements. An enhancement of 200% was noticed in the single-phase regime and since the two-phase regime was delayed, a heat transfer enhancement of up to 181% was achieved. Interestingly, the onset of the two-phase regime was found to occur at a temperature that was independent of the nozzle pressure and mass flow rate. Duursma *et al.* (2009) conducted an investigation of the droplet impinging mechanics using dimethyl sulfoxide (DMSO) and ethanol nanofluids. The nanoparticles used in the investigation where aluminum with mass concentrations of up to 0.1% for DMSO and 3.2% for ethanol. Single droplets where impinged onto the surface where high-speed photographic images were taken to show the differences in

droplet behavior. The results revealed that droplet mechanics are mostly a function of Weber number and excess temperature. An increase in the nanoparticle concentration results in a decrease in the droplet breakup on rebound after impingement and reduces the spreading of the droplet as well. The maximum recoil height in also reduced with increasing mass concentration. The heat fluxes of the pure bulk fluids and the ethanol nanofluids did not show any significant enhancement. The DMSO nanofluid did show significant enhancement in heat flux when compared to the bulk fluid. Sefiane *et al.* (2009) researched the evaporation kinetics and wetting dynamics on rough heated surfaces of alumina oxide nanoparticles suspended in ethanol. The experiment looked at the shape of the droplets by measuring the contact angle, base diameter, and volume as a function of time. The pinning of the drops on the heated surface became very important factor. The ethanol with nanoparticles took a longer period of time to pin itself to the solid surface and therefore lead to a decrease in evaporation rate when compared to the base fluid alone. The contact angles for the nanofluid were found to be larger during the depinning process than for the base fluid. The total evaporation time was found to be longer for the base fluid compared to the nanofluid. Again, contrary to the increase in thermal conductivity and heat transfer coefficient, the addition of nanoparticles has had an adverse effect on phase change heat transfer.

Table 1: Summary Table

	Enhancing Effects	Deteriorating Effects	References
pH Effects			
Keep pH level away from isoelectric point	Increases the dispersion of nanoparticles, hydration forces and ability for heat		Anoop *et al.* (2009)

Table 1: Summary Table (Continued)

Increase in pH level		Thermal conductivity ratio decreases	Xie *et al.* (2002)
Transient Hot Wire Method			
Nanoparticle volume fraction	Higher volume fraction results in an increase in thermal conductivity		Xuan *et al.* (2000)
Base fluid thermal conductivity	Lower thermal conductivity fluids will benefit more from the addition of nanoparticles	Fluids with high thermal conductivities will benefit little from the addition of nanoparticles	Hwang *et al.* (2006)
Nanoparticle thermal conductivity and thermal diffusivity dependence on temperature		Does not have an effect on the thermal conductivity of the nanofluid	Zhang *et al.* (2006)
Nanoparticle surface area	An optimum specific surface area exist		Xie *et al.* (2002)
Pool Boiling			
Delay of nucleate boiling regime		Inconsistent with the increase of thermal conductivity of nanofluids	Bang *et al.* (2005)
Fouling of the heated surface by nanoparticles		Decrease in nucleation site density	Bang *et al.* (2005)
CHF enhancement		Not related to the increase in thermal conductivity by the addition of nanoparticles	You *et al.* (2003)
Increase in viscosity of the base fluid by the addition of nanoparticles	Increase in heat transfer of the base fluid		Das *et al.* (2003)
Decrease in nucleation site density		Overshadows the increase in heat transfer	Das *et al.* (2003)

Table 1: Summary Table (Continued)

Very small addition of nanoparticles		No effect on boiling heat transfer	Trisaksri *et al.* (2009)
Deposition of nanoparticles on surface		Introduces a thermal resistance	Wen *et al.* (2008)
Increase in wettability	Driving mechanism for increase in CHF		Coursey *et al.* (2008)
Impinging Jet			
Nanoparticle concentration, flow rate, and nozzle-to-surface distance	There exist an optimum to give the best results		Nguyen *et al.* (2009)
Jet boiling curves shifted to the right when using nanofluids		Indicates a deterioration of boiling heat transfer	Liu *et al.* (2007)
Surface became smoother after using nanofluids		Decrease in boiling heat transfer	Liu *et al.* (2007)
Prevention of vapor blanket formation by the trapping of liquid in the porous layer	Increase in the CHF		Liu *et al.* (2007)
Spray Cooling			
Nanoparticle addition reduces evaporation time	Enhancement to heat transfer for evaporative cooling		Shen (2009)
Addition of high aspect ratio microchannels to the copper surface	200% enhancement to single-phase heat transfer and 181% enhancement to two-phase heat transfer		Coursey (2007)
Longer evaporation time for the base fluid compared to the nanofluid	Heat transfer enhancement		Sefiane *et al.* (2009)

Chapter 4 – Experimental Setup and Procedure

4.1 Nanofluid Preparation

In the current study, Al_2O_3 nanoparticles were chosen because of their widely known thermal properties and ease of dispersion in de-ionized water. Aluminum Oxide mass concentrations of 0.1%, 0.5% and 1% were used for the investigation. The nanoparticles used were made by Nanophase Technologies Corporation. The properties of the nanoparticles are:

Table 2: Properties of Aluminum Oxide Nanoparticles

Purity	Avg. Particle Size	Specific Surface Area	True Density	Morphology
99.5+%	45 nm	45 m^2/g	3.6 g/cc	Spherical

The mass of the de-ionized water was determined on a digital scale at which time the desired mass concentration of alumina nanoparticles was added. Initial dispersion of the mixture was achieved by sonicating the mixture for a minimum of 12 hours by the use of an Ultrasonic Cleaner FS140 sonicator. Some evaporation of the nanofluid occurred due to the temperature rise during sonication. To prevent any significant loss of de-ionized water mass, a lid was placed on the container and any change to the nanofluid mass concentration was assumed to be insignificant. To assure proper alumina nanoparticle dispersion during the experiment, the pH of the sonicated nanofluid was altered. An Oakton pH 11 handheld pH meter was used to determine the pH level of the nanofluid.

Since pH levels are a function of temperature, the container of hot nanofluids was taken from the sonicator and placed in a pool of room temperature water. Once equilibrium was achieved the pH level of the nanofluid was changed with the use of sodium hydroxide (NaOH) and hydrochloric acid (HCl). The pH levels for the different mass concentrations of alumina nanofluids were determined from the work of Anoop *et al.* Though the investigation that was referenced only dealt with mass concentrations of 1%, 2%, 4%, and 6%, the data was plotted and extrapolated to apply to the current investigation. The result of the regression yielded:

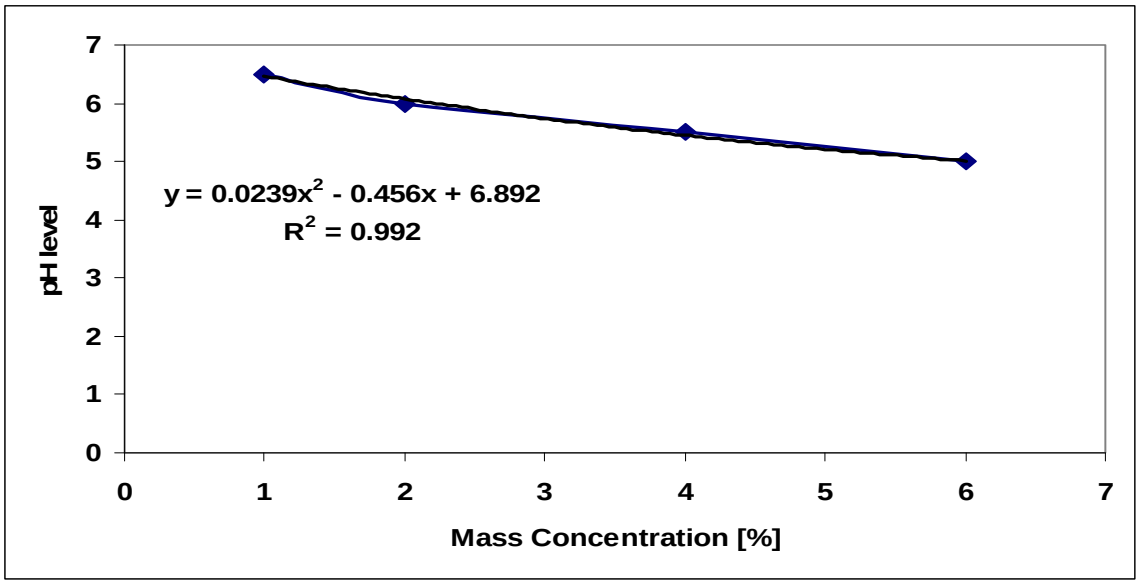

Figure 1: pH Level vs. Mass Concentration of Alumina Nanofluids

The extrapolated data gave pH values of:

Table 3: pH Level of Selected Mass Concentrations

Mass Concentration	pH Level
0.1%	6.8
0.5%	6.7
1.0%	6.5

Visual inspection of the nanofluid after pH alteration showed that after 5 days the alumina nanoparticles maintained good dispersion within the water. This was noticed by the cloudiness of the nanofluid, especially noticeable near the surface of the container. If the nanofluid was clearer near the top of the container it was assumed that the nanoparticles were not very well dispersed.

4.2 Copper Block

The copper block was fabricated out of single piece of tellurium copper. Tellurium copper was chosen for this investigation because of its high thermal conductivity and machinability. A 25.4 mm^2 heated surface was fabricated for this investigation. The copper block was designed to provide a 40.64 mm long extended surface where three K-type, 30 gage thermocouples were inserted 12.7 mm deep at distances of 1 mm, 11 mm, and 21 mm from the spray surface. The base of the copper block was 76.2 x 76.2 x 50.8 mm and had five holes fabricated where cartridge heaters were inserted.

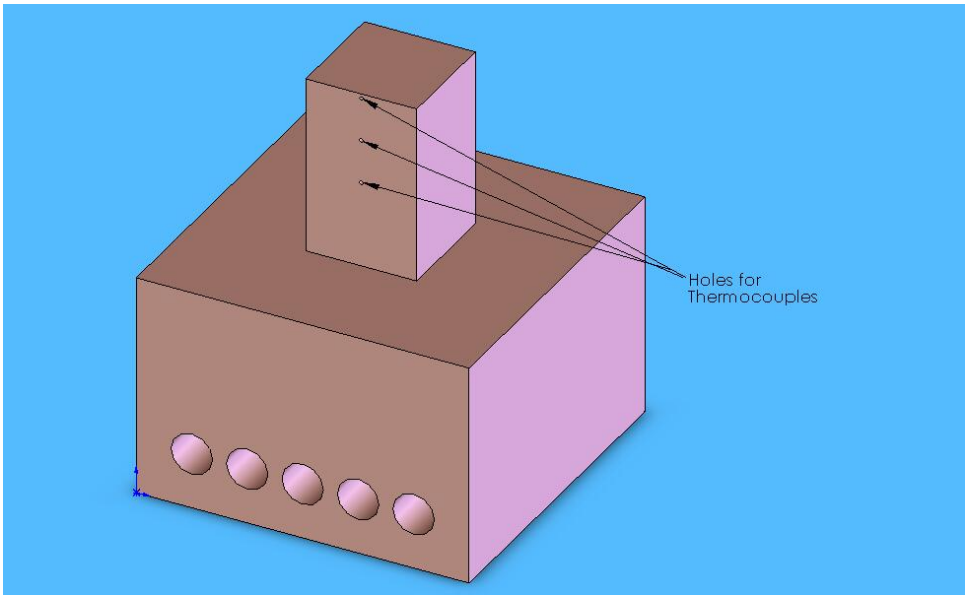

Figure 2: Copper Block Design

The OMEGALUX CIR-2013/120V cartridge heaters were 50.8 mm long with a 9.525 mm diameter and had a rated wattage of 500 watts. Through prior experimentation, it was found that only four cartridge heaters were needed to conduct the investigation. The cartridge heaters where inserted at the ends leaving the center hole empty. Due to the high temperatures produced in the copper block an insulation of concrete was molded and placed on the extended surface. Concrete was chosen because of its minimum expansion with temperature rise, cost effectiveness, could be easily reproduced in the laboratory and it sufficiently insulated the extended surface for the current investigation. An insulated surface was necessary to justify assumption of a linear temperature profile. To validate the assumption of a linear temperature profile through the extended surface and a uniform heat flux at the spray surface a COMSOL model was developed. The boundaries of the model experienced convective heat transfer at 293 K and a convective heat transfer coefficient of 40 W/m^{2}K. The material properties of the concrete insulation were given by COMSOL's materials database. The volumetric heat flux (q'''), generated by the cartridge heaters, was found by the following equation:

$$q''' = \left(P_R \times \frac{V_A^2}{V_R^2} \right) \times \frac{1}{\lambda_C},$$

where P_R is the rated wattage of the cartridge heaters, V_A is the actual voltage, V_R is the rated voltage and λ_C is the circumferential volume of the cartridge heaters. The following figure demonstrates the boundary temperature profile for the copper block with 15 volts of actual voltage to the cartridge heaters:

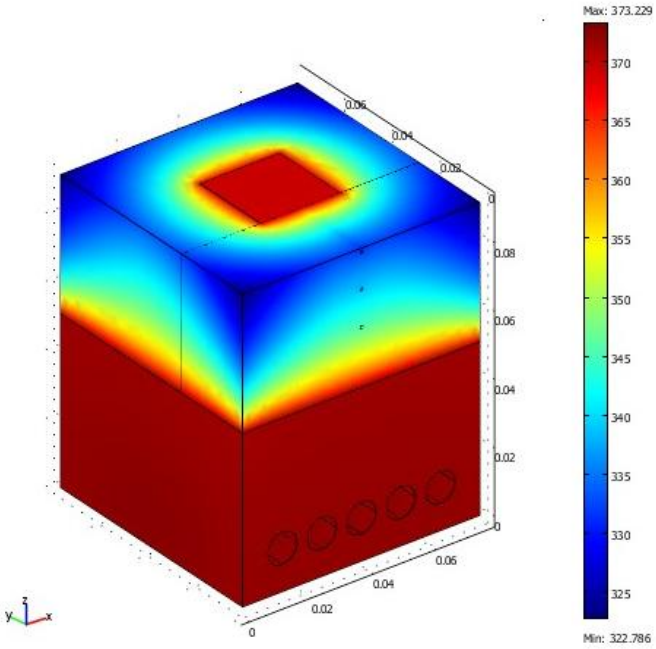

Figure 3: Boundary Temperature Profile

The heat flux path is shown to be linear through the extended surface of the copper block.

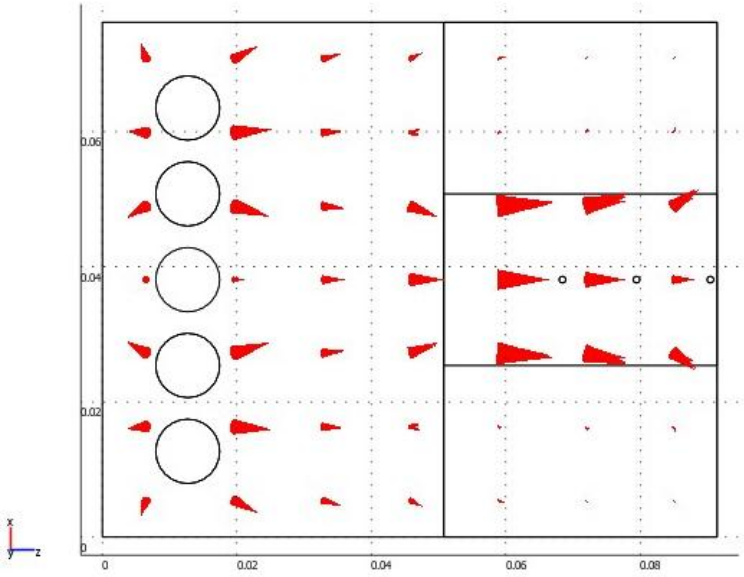

Figure 4: Heat Flux Path through Block

A uniform heat flux normal to the spray surface is important for accurate calculations during the experiment. The model shows that the insulation adequately provides this uniformity.

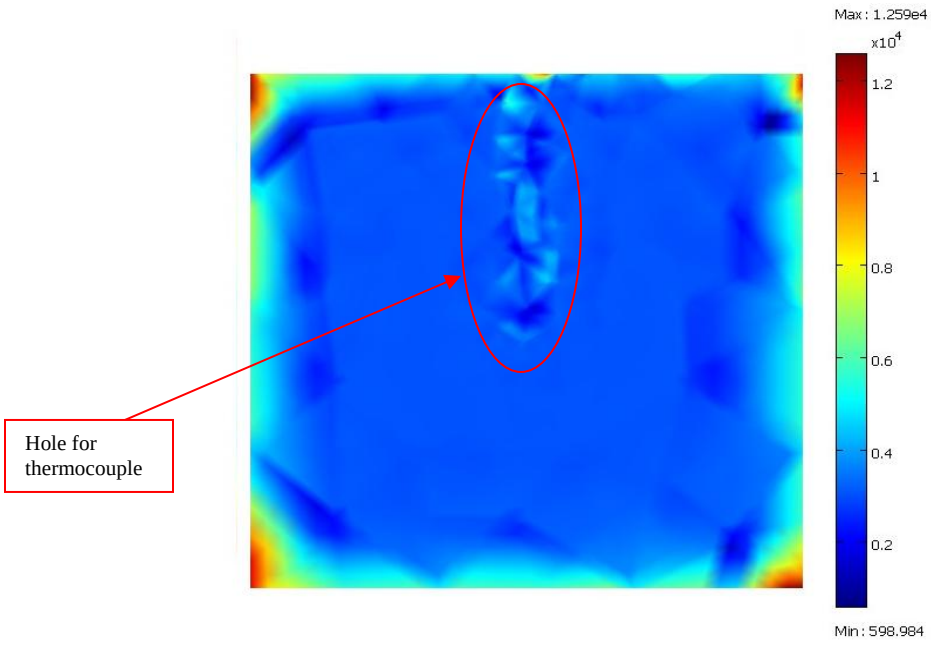

Figure 5: Heat Flux Normal to Spray Surface

4.3 Spray System

The working fluid was poured into a pressure tank that was pressurized by a compressed nitrogen tank. The flow of the working fluid was regulated by a flow meter connected to a Tefen standard conical spray nozzle.

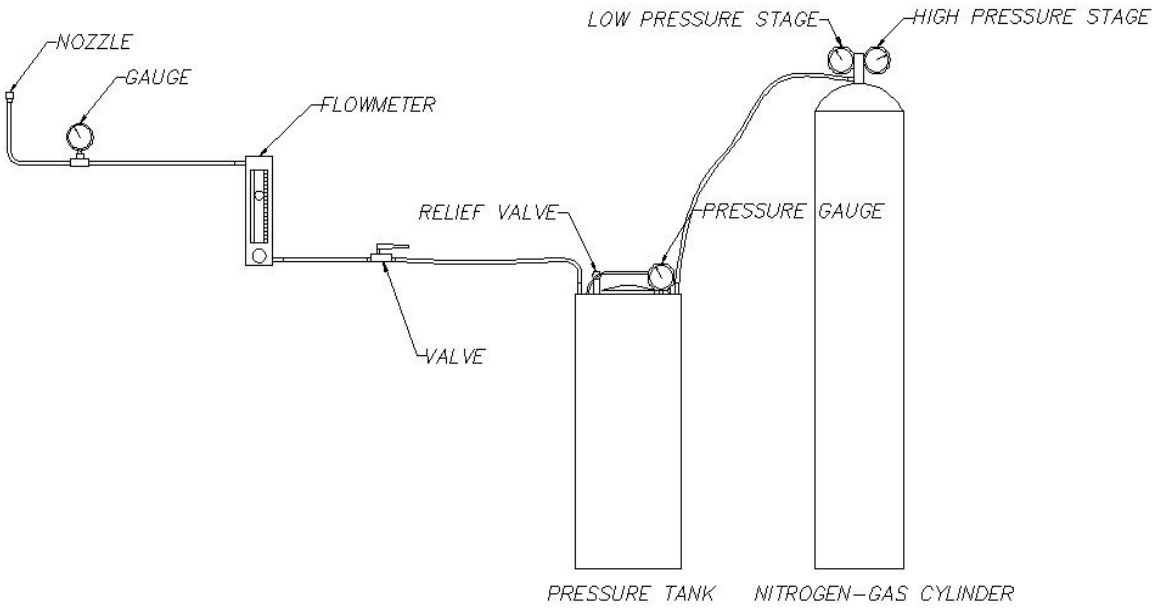

Figure 6: Schematic of Spray System

The nozzle was designed to deliver a uniform size and distribution of the droplets. The distance between the nozzle and the heated surface was maintained at 21 mm. The mass flow rates used in this investigation were:

Table 4: Mass Flow Rates

Pressure [psi]	Mass flow rate [g/s]
40	0.53
45	0.58
50	0.61

4.4 Spray Surface Preparation

The heated copper surface was cleaned after every trial to ensure that the surface characteristics were maintained relatively unchanged from one trial to the next. After spray cooling with both water and the nanofluids, thin films were observed on the heated surface. A layer of oxidation was caused by the water and a thin film of alumina nanoparticles were deposited by the nanofluid. After the copper block was allowed to

reach room temperature a liberal amount of Vishay Measurements Group, Inc. M-PREP conditioner was placed on the spray surface and wet-lapped 20 times in the same direction with 320 grit sandpaper to ensure uniformity of the surface. A clean gauze was used to dry the surface after wet-lapping. Finally, M-PREP neutralizer was applied with clean cotton-tipped applicators and the surface was dried once again.

4.5 Acquisition System

A computer with an acquisition system made by National Instruments was used to acquire data for this investigation. The thermocouples were connected to a NI SCXI-1303 terminal block. This block is designed specifically for high-accuracy thermocouple measurements and minimizes errors by using an isothermal construction. The data was displayed on the computer by the use of LabVIEW 7.1 software. A program was written that would display the temperature of each thermocouple simultaneously as a function of time.

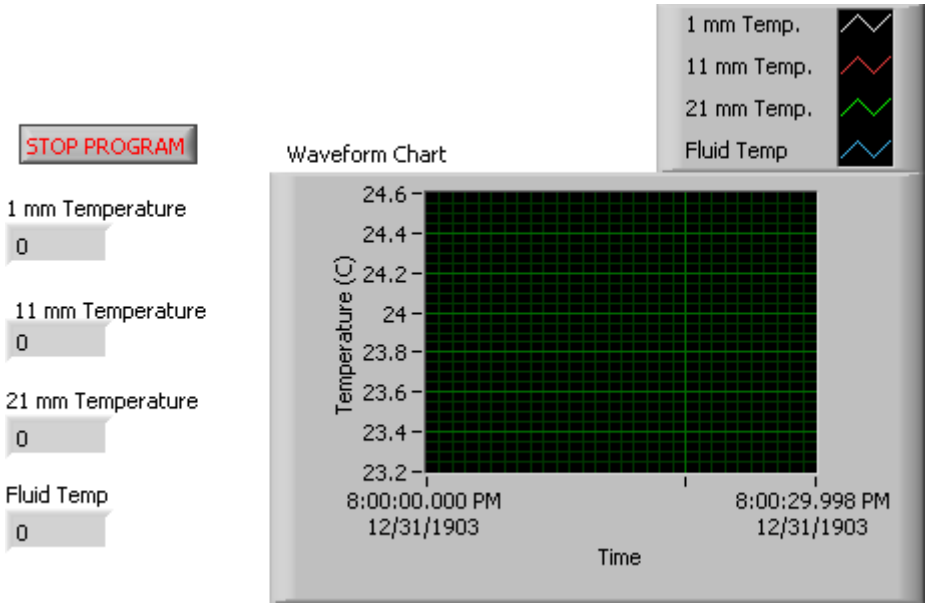

Figure 7: LabVIEW Front Panel

The waveform chart was used to determine when a steady state condition had been reached. The resolution of the program was 1 sample at a rate of 10 Hz, which gave a good description of the measured transient temperatures data.

4.6 Surface Roughness Measurement

To study the effects on the surface by spray cooling with nanofluids, measurements of its surface roughness were made. To measure the roughness profile a Surtronic 3P profilometer was used. The profilometer used a diamond tip stylus with a diameter of 5 μm. The profilometer was able to compute and display common surface roughness values. The cutoff length of the profilometer was 0.8 mm. That meant that the profilometer could not detect any deviation from the normalized data greater than 0.8mm.

4.7 Experimental Procedure

The experimental setup consisted of an open spray system and the copper block was oriented horizontally on a metal stand. The effectiveness of different mass concentrations of alumina nanofluids were compared to de-ionized water at the same nozzle pressure and distance from the heated surface. The experimental procedure was repeated three times at each concentration and pressure to arrive at an average. The mass of the de-ionized water was measured and the required alumina nanoparticles were added to achieve the desired mass concentration. The mixture was then sonicated for at least 12 hours to disperse the nanoparticles. After sonication, the mixture was allowed to reach a temperature of 25 ˚C in a cooling bath. The pH of the nanofluid was altered to maintain the nanoparticles in dispersion for the duration of the experiment. The nanofluid was poured into the pressure tank and the desired spray nozzle pressure was set by using the compressed nitrogen tank. The thermocouples were inserted into the extended surface of the copper block and the insulation was placed. The electrical cartridge heaters were inserted into the copper block base and energized. The flow meter was fully opened and the spray cooling of the surface began. Once steady state was achieved, the temperatures of the three thermocouples were recorded and the voltage to the cartridge heaters was increased gradually until critical heat flux (CHF) was reached. After concluding the experiment, the thermocouples, insulation, and cartridge heaters were removed and the copper block was allowed to cool. Once cooled, the spray surface was cleaned and prepared for the next experiment.

Chapter 5 – Results and Discussion

5.1 Uncertainty Analysis

In the current investigation, the uncertainties of the heat-flux calculations were dependent on the uncertainty of the temperature readings and the distance between the thermocouples. To measure the uncertainty of the temperature readings, the uncertainty of the thermocouples and the DAQ (Data Acquisition) board became important. First, the uncertainty of the thermocouples had to be expressed in terms of a voltage. The sensitivity (S_{TC}) of the thermocouple was found by dividing the thermoelectric voltage (V_{TE}) of the thermocouple by the corresponding temperature (T).

$$S_{TC} = \frac{V_{TE}[mV]}{T[^{\circ}C]}$$

To find the uncertainty of the thermocouple in terms of voltage ($U_{TC,V}$), the sensitivity was then multiplied by the uncertainty of the thermocouple ($U_{TC,T}$) in degrees Celsius, which was 2.2 ˚C.

$$U_{TC,V} = S_{TC}\left[\frac{mV}{^{\circ}C}\right] \times U_{TC,T}[^{\circ}C]$$

The uncertainty of the DAQ board (U_{DAQ}) was found by dividing the voltage range (V_R) by 2 raised to the resolution of the board, which was 16 bits.

$$U_{DAQ} = \frac{V_R[mV]}{2^{16}}$$

With the uncertainty of the thermocouple and the DAQ board both in terms of voltages, the voltage uncertainty of the readings (U_V) could be found by:

$$U_V = \sqrt{(U_{TC,V})^2 + (U_{DAQ})^2}$$

Finally, the uncertainties of the temperature readings (U_T) were found by converting the voltage uncertainty (U_V) using the scaling function in the LabVIEW software. The scaling function is used by LabVIEW to convert a measured voltage to temperature. The conversion was given by:

$$\begin{aligned} U_T = U_V * ((2.508355E\text{-}2) + U_V * ((7.860106E\text{-}8) + \\ U_V * ((-2.503131E\text{-}10) + U_V * ((8.315270E\text{-}14) + \\ U_V * ((-1.228034E\text{-}17) + U_V * ((9.804036E\text{-}22) + \\ U_V * ((-4.413030E\text{-}26) + U_V * ((1.057734E\text{-}30) + \\ U_V * (-1.052755E\text{-}35)))))))) \end{aligned}$$

The scaling function has a range of 0 ˚C to 500 ˚C. The distance between the thermocouples was found by a caliper with a resolution of 0.001 meters. Therefore, the uncertainty of the distance (U_C) was found by taking half the resolution.

$$U_c = \frac{0.001m}{2} = 0.0005m$$

The uncertainty of the heat flux ($U_{q"}$) was found by considering the uncertainties of the temperature readings (U_T) and the distance between the thermocouples (U_C).

$$U_{q"} = q \times \sqrt{\left(\frac{U_T^2}{\Delta T}\right)^2 + \left(\frac{U_C}{L}\right)^2},$$

where q is the calculated heat flux between the thermocouples at 1 mm and 11 mm from the heated surface, ΔT is the temperature difference between the two thermocouples, L is

the distance between the thermocouples, U_C is the uncertainty of the distance between the two thermocouples, and U^2_T is the temperature uncertainty of the temperature difference between the thermocouples and is given by:

$$U_T^2 = \sqrt{(U_{T,1})^2 + (U_{T,11})^2},$$

where $U_{T,1}$ and $U_{T,11}$ are the temperature uncertainties at distances of 1 mm and 11 mm from the heated surface respectively. The uncertainty analysis revealed that the uncertainty of the heat flux measurements were approximately $\pm 4.6\%$.

5.2 Experimental Results

In this investigation the heat flux removed from the heated surface was calculated by using one-dimensional conduction through the extended surface:

$$q'' = -k \times \left(\frac{\Delta T_{1..11}}{L_{1..11}} \right)$$

where k is the thermal conductivity of the copper block, $\Delta T_{1..11}$ is the temperature difference between thermocouples at distances of 1 mm and 11 mm from the heated surface, and $L_{1..11}$ is the distance between the thermocouples. The heat flux was plotted against the temperature of the surface minus the temperature of the working fluid. The temperature of the working fluid was approximately a constant 23.5 ˚C throughout the length of the experiment. To find the temperature of the surface the heat flux calculated between the thermocouples at 1 mm and 11 mm from the surface was assumed to be equal to the heat flux between the surface and the first thermocouple. Therefore, the surface temperature could be calculated by:

$$T_S = \left(\frac{q''}{-k} \times L_{S..1} \right) + T_1$$

where q'' is the calculated heat flux, k is the thermal conductivity of the copper, $L_{S..1}$ is the distance between the surface and the first thermocouple and T_1 is the temperature of the thermocouple at 1 mm from the surface. De-ionized water was first investigated at the different operating pressures. The results of the de-ionized water spray cooling heat transfer curves were compared to investigate the role of pressure on heat transfer.

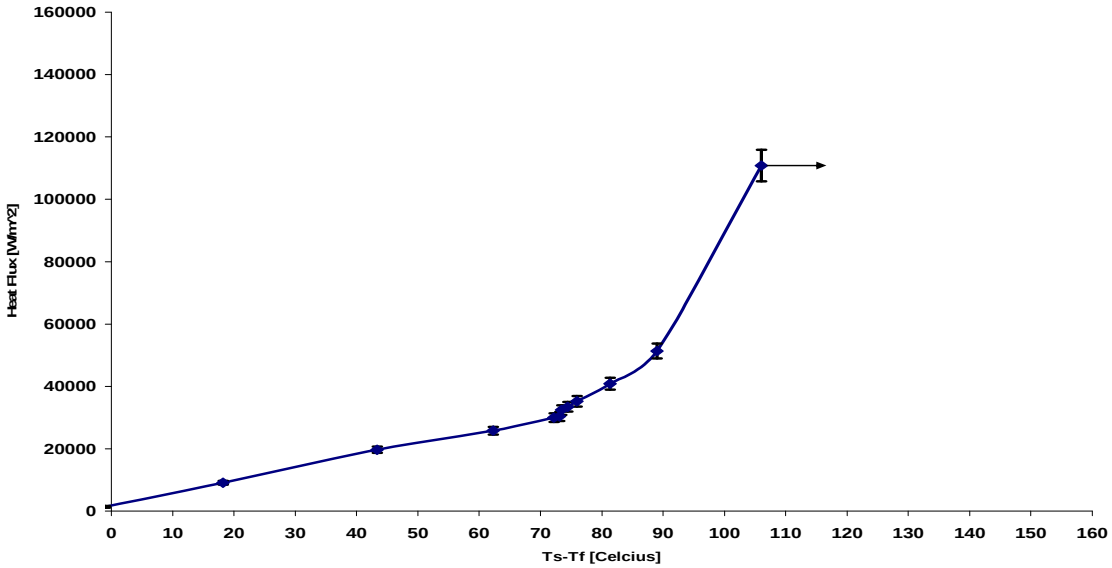

Figure 8: Spray Cooling Curve for Water at 40 Psi

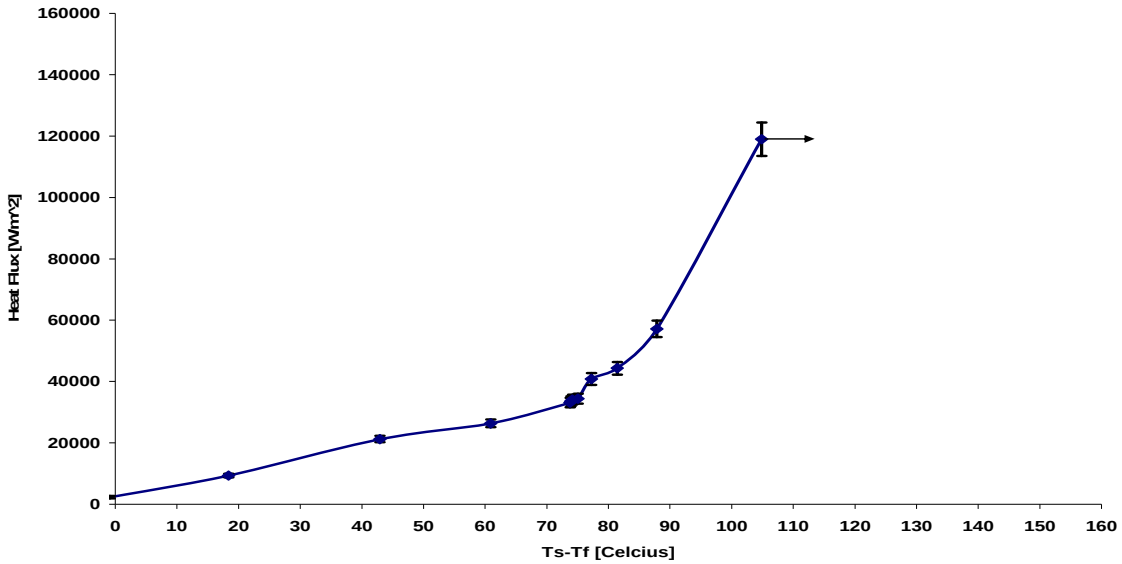

Figure 9: Spray Cooling Curve for Water at 45 Psi

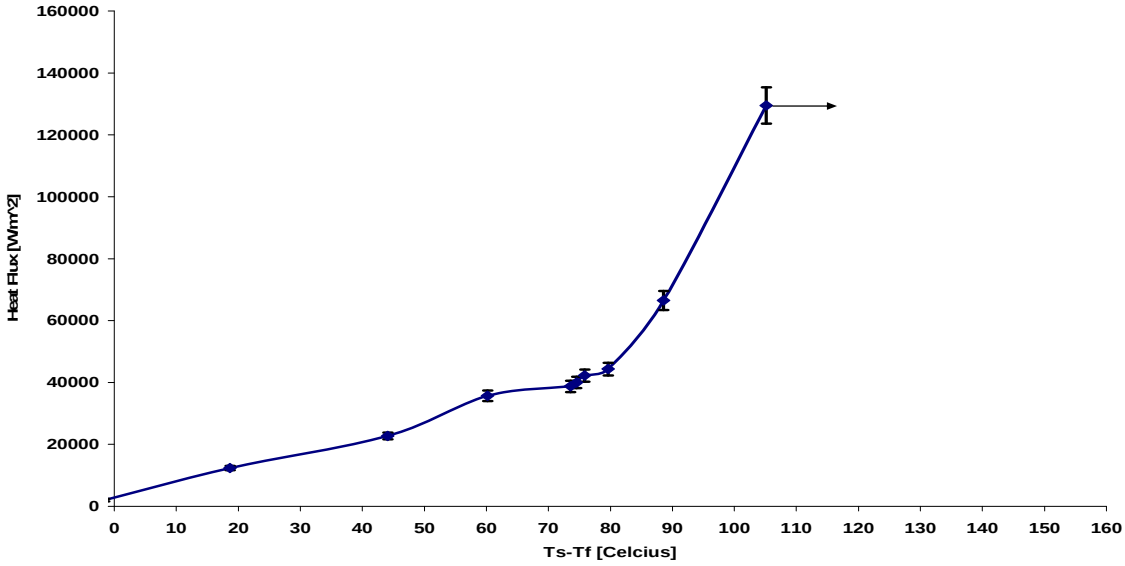

Figure 10: Spray Cooling Curve for Water at 50 Psi

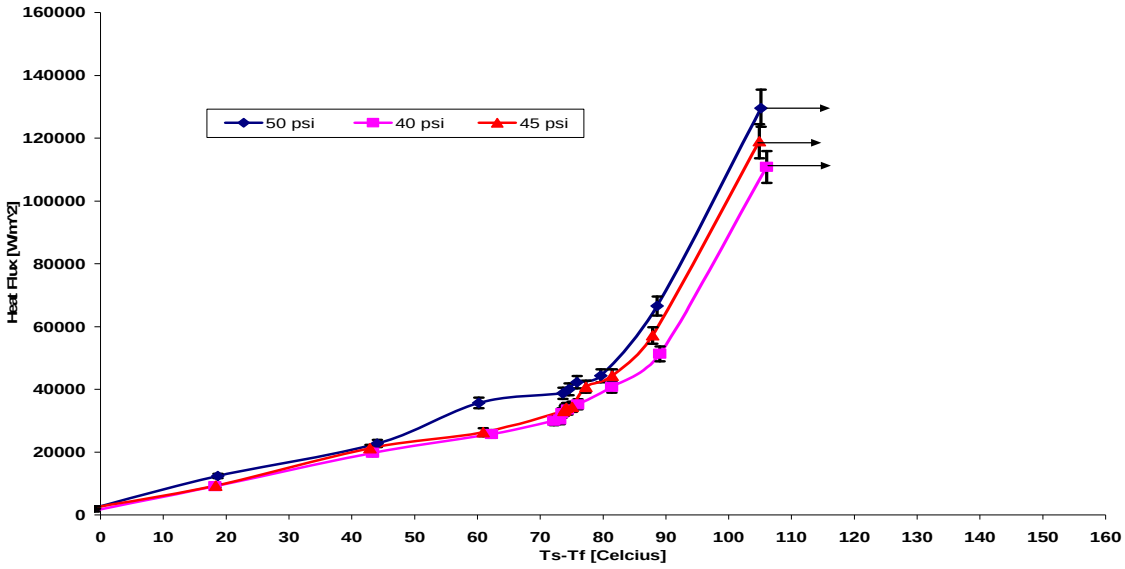

Figure 11: Spray Cooling Curve Comparison of Water at Different Pressures

Comparing the spray cooling heat transfer curves of water at the three different pressures showed that with increasing pressure, the heat transfer at the surface also increased. These results were expected because when the pressure is increased it results in an increase in the mass flow rate of water droplets being delivered to the heated surface. The CHF values at the corresponding temperatures are given below:

Table 5: Critical Heat Flux for Water

Pressure [Psi]	Critical Heat Flux [W/m^2]	Temperature [Celsius]
40	110,833	106
45	119,000	104.8
50	129,500	105.1

The data shows that increasing the pressure results in an increase in the CHF by 7.4% and 8.8% when going from 40 to 45 Psi and 45 to 50 Psi respectively. After the completion of the water data, one of the four cartridge heaters malfunctioned. The experiments for the nanofluid part of the investigation was done with only three cartridge heaters, one inserted in the center and one on either side. As a result of using only three cartridge

heaters, more data points were collected during the spray cooling experiments with nanofluids. With only three cartridge heaters the heat flux generated at the same variac voltage was insufficient to reach CHF. Therefore, the number of times the variac was incrementally increased to reach CHF was higher with three cartridge heaters than with four.

The investigation began by looking at 1.0% mass concentration of alumina nanofluid.

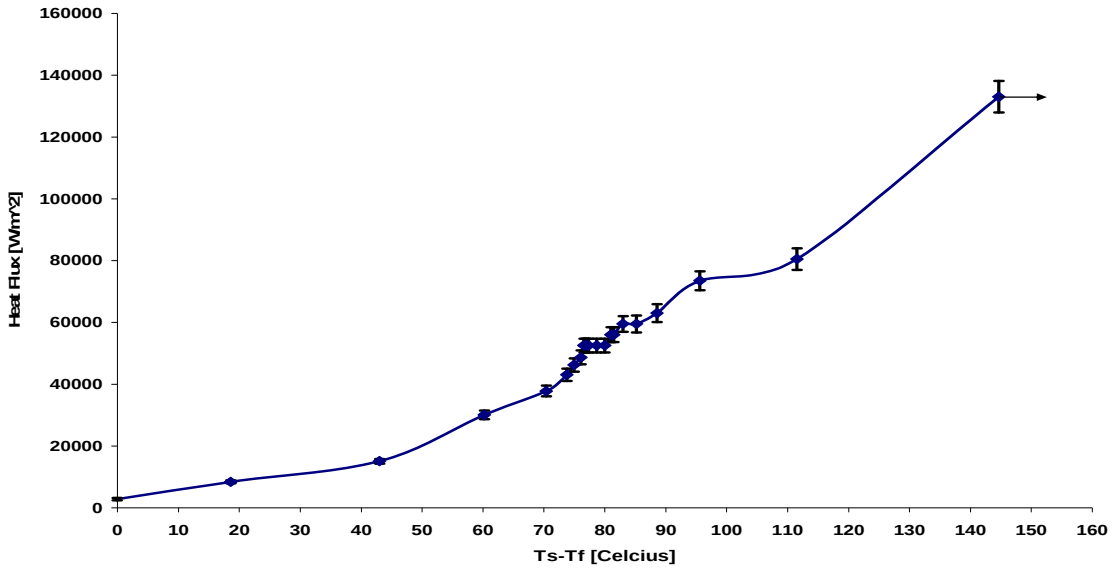

Figure 12: Spray Cooling Curve for 1.0% wt. Alumina Nanofluid at 40 Psi

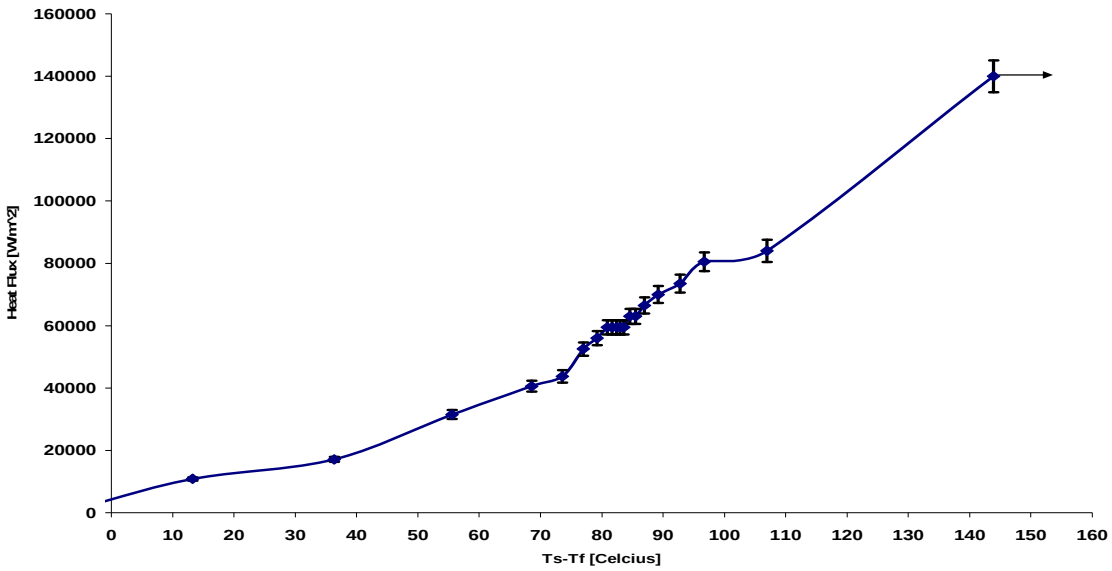

Figure 13: Spray Cooling Curve for 1.0% wt. Alumina Nanofluid at 45 Psi

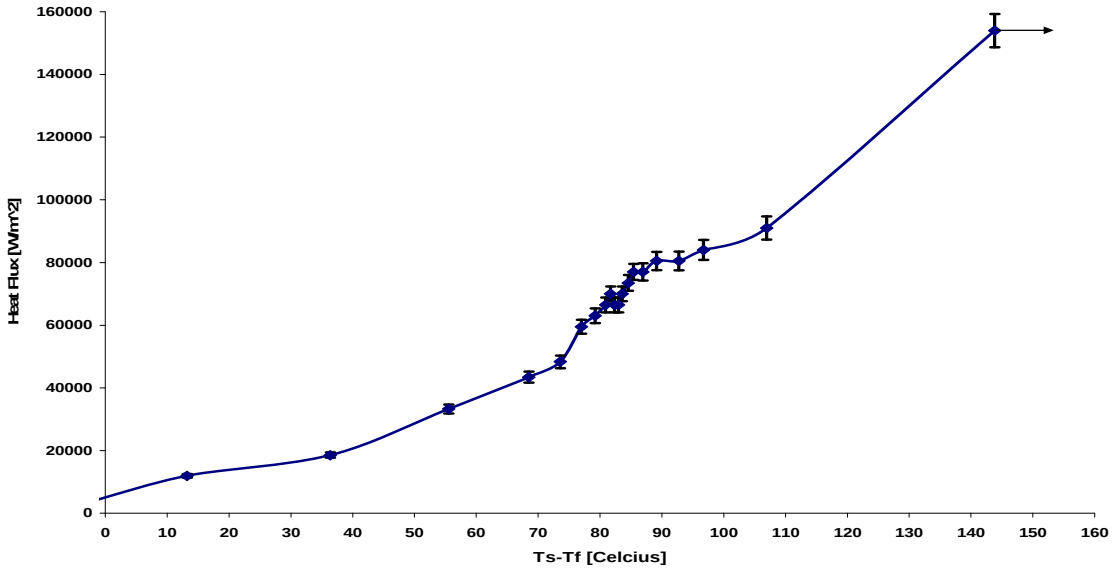

Figure 14: Spray Cooling Curve for 1.0% wt. Alumina Nanofluid at 50 Psi

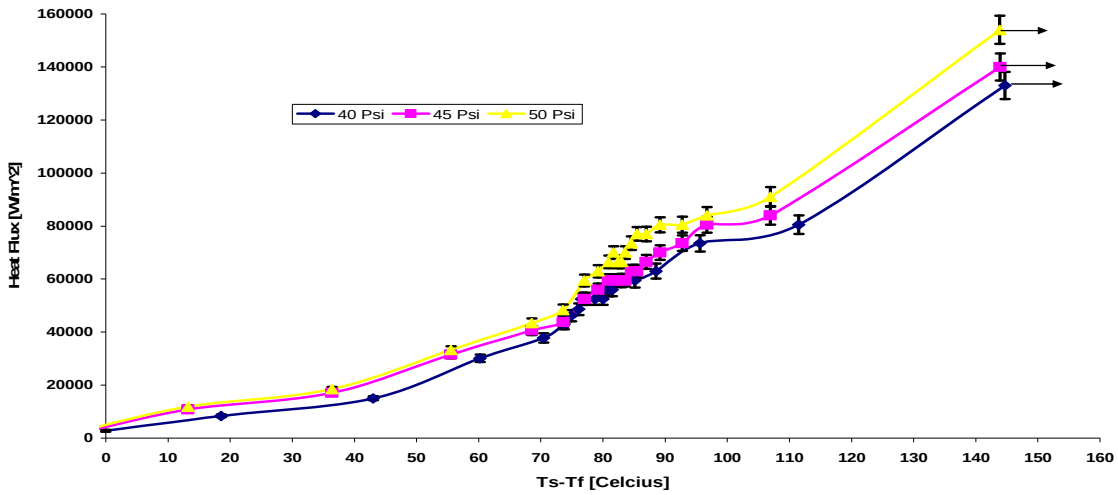

Figure 15: Spray Cooling Curve Comparison of 1.0% wt. Alumina Nanofluid at Different Pressures

Similar to the results obtained for water, the heat flux obtained by using alumina nanofluids increased with increasing pressure. The CHF values at the corresponding temperature for each pressure are given below:

Table 6: Critical Heat Flux for 1.0% wt. Alumina Nanofluids

Pressure [Psi]	Critical Heat Flux [W/m^2]	Temperature [Celsius]
40	133,000	144.7
45	140,000	143.9
50	154,000	143.8

An increase in the CFH of 10% resulted from an increase in pressure from 45 to 50 Psi compared to only a 5.3% increase when increasing the pressure from 40 to 45 Psi. The results for 0.5% wt. concentrations are shown below.

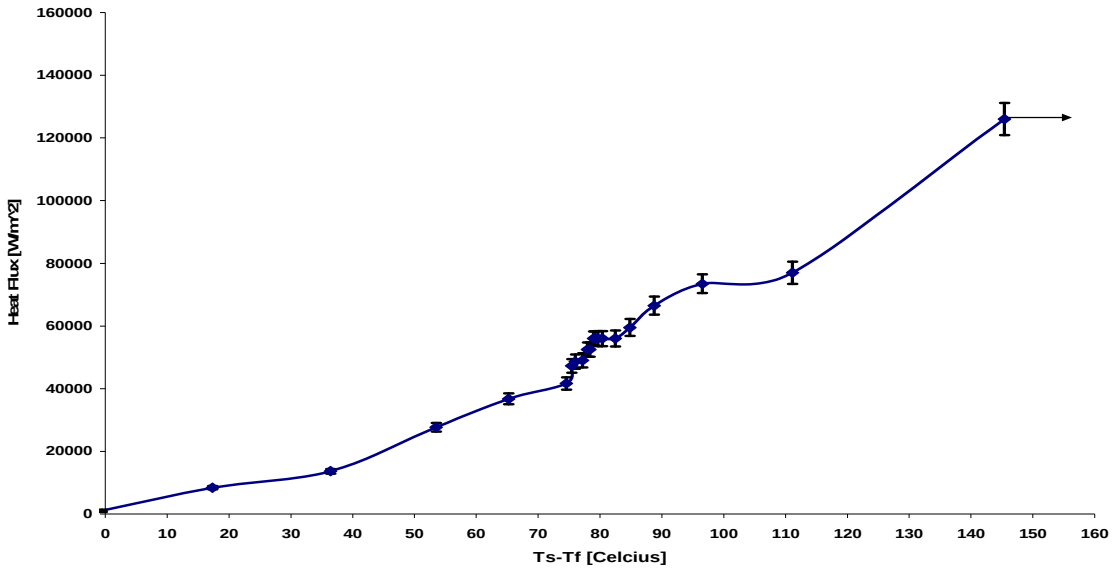

Figure 16: Spray Cooling Curve for 0.5% wt. Alumina Nanofluid at 40 Psi

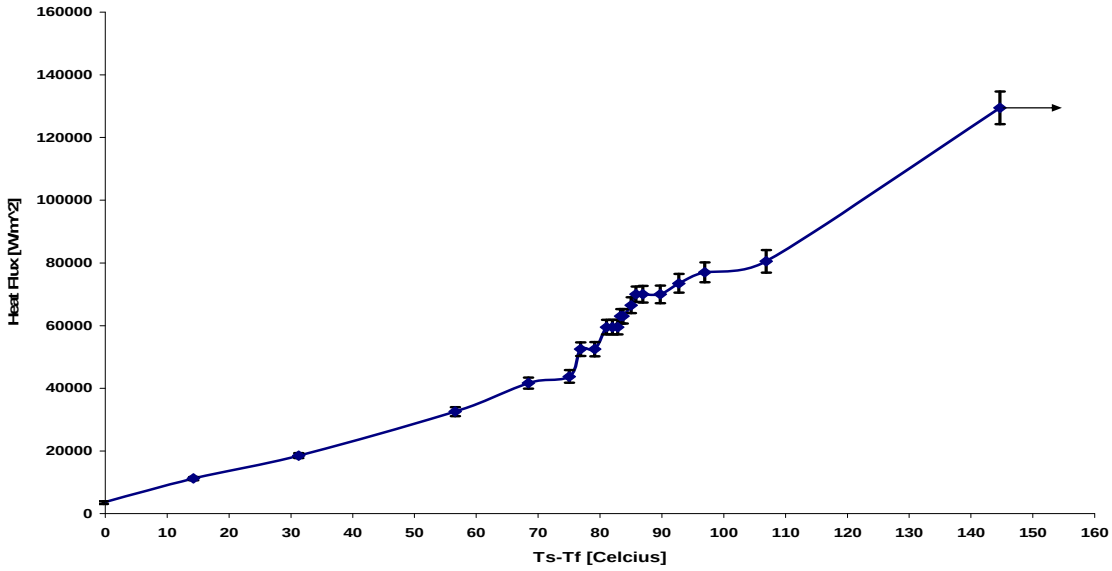

Figure 17: Spray Cooling Curve for 0.5% wt. Alumina Nanofluid at 45 Psi

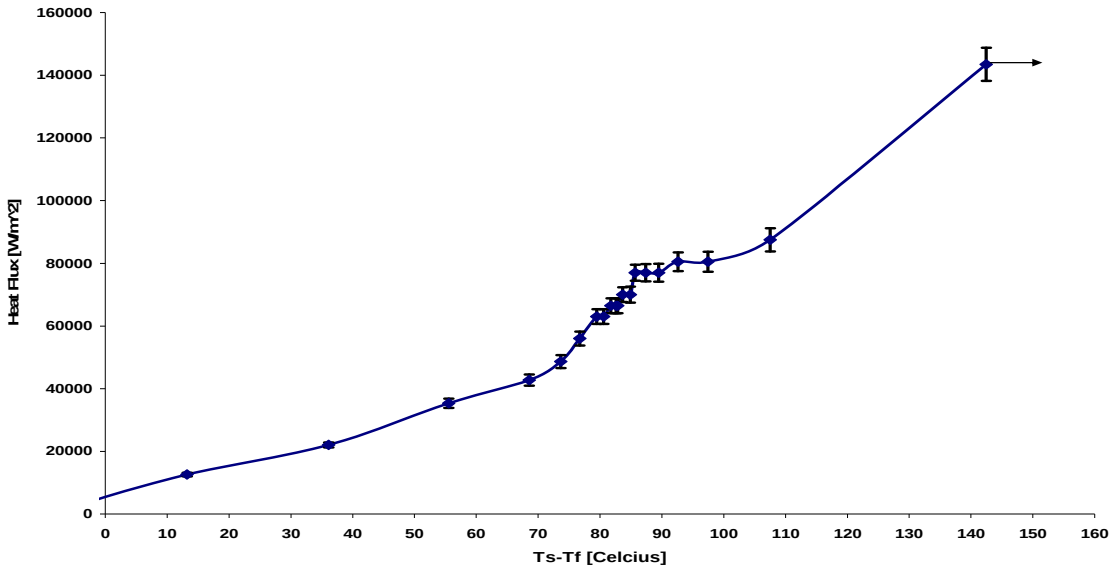

Figure 18: Spray Cooling Curve for 0.5% wt. Alumina Nanofluid at 50 Psi

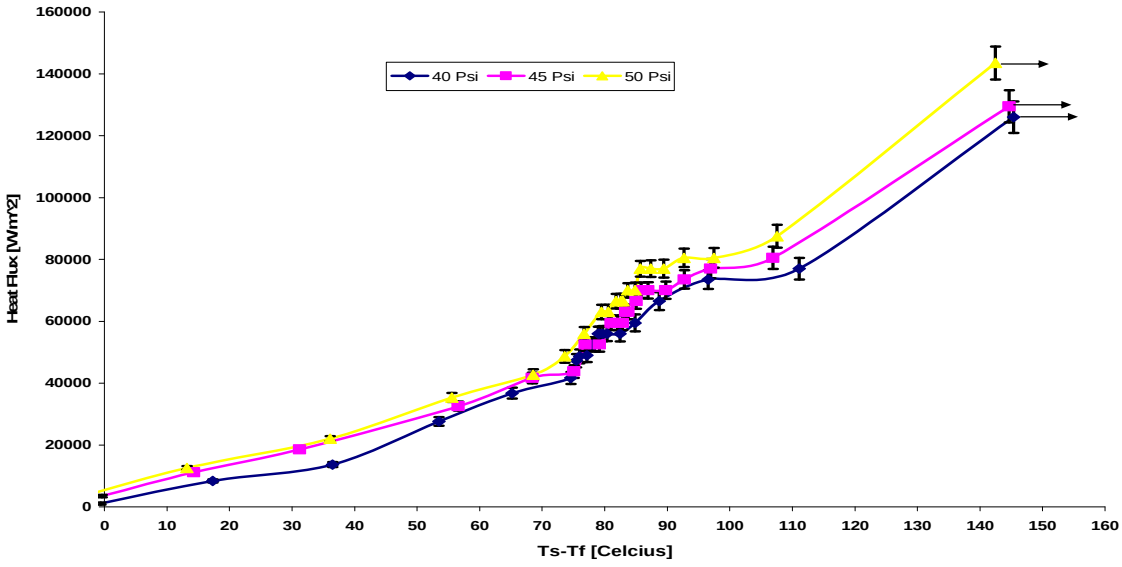

Figure 19: Spray Cooling Curve Comparison for 0.5% wt. Alumina Nanofluids at Different Pressures

As expected, the increase in pressure causes an increase in the heat flux removed from the heated surface. The CHF values at the corresponding temperatures for each pressure are given below:

Table 7: Critical Heat Flux for 0.5% wt. Alumina Nanofluid

Pressure [Psi]	Critical Heat Flux [W/m^2]	Temperature [Celsius]
40	126,000	145.4
45	129,500	144.7
50	143,500	142.5

Increasing the pressure from 40 to 45 Psi only yielded a 2.8% increase in the CHF for 0.5% wt. alumina nanofluid. A more significant increase of 10.8% was noticed in the CHF when the pressured was raised from 45 to 50 Psi. Finally, the 0.1% wt. concentration results are given below.

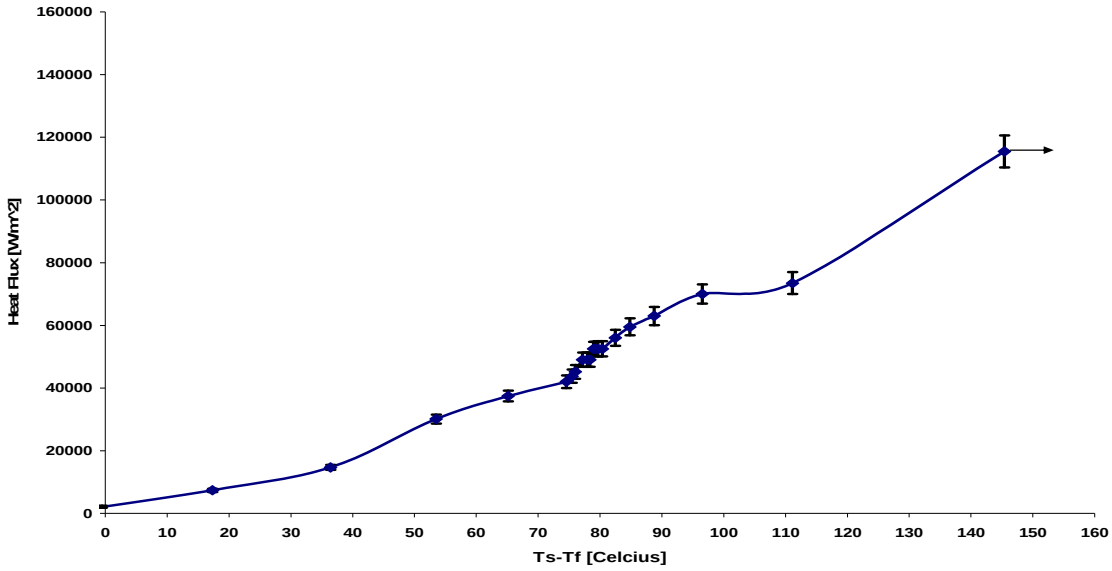

Figure 20: Spray Cooling Curve for 0.1% wt. Alumina Nanofluid at 40 Psi

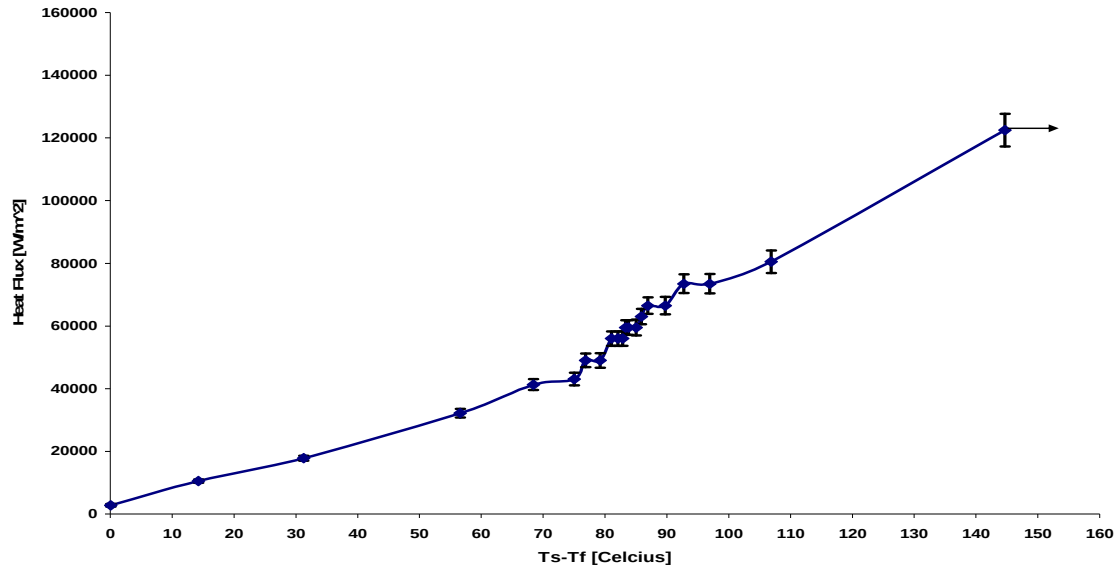

Figure 21: Spray Cooling Curve for 0.1% wt. Alumina Nanofluid at 45 Psi

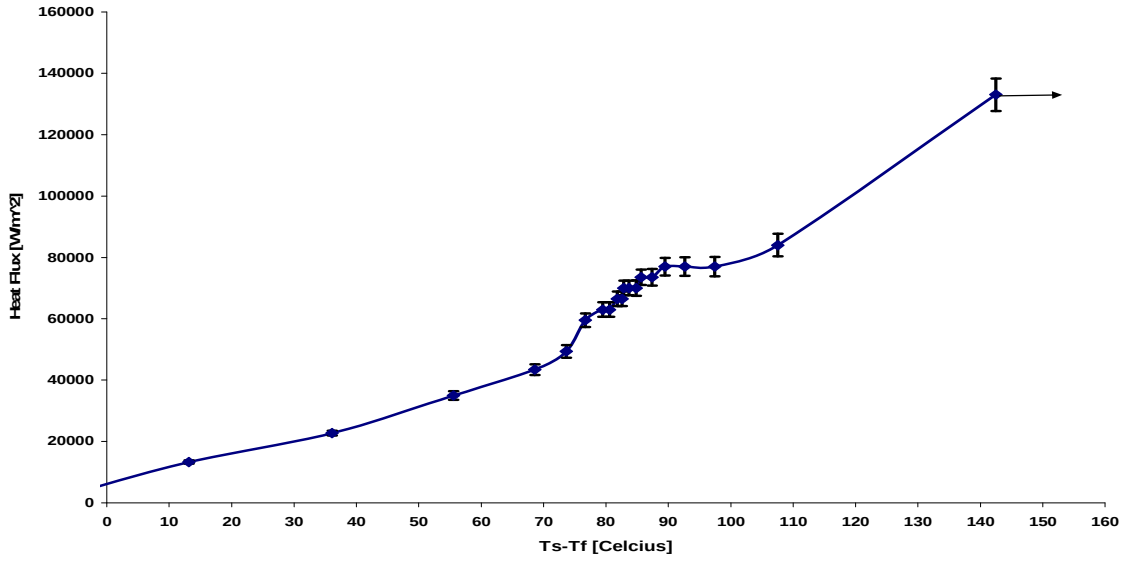

Figure 22: Spray Cooling Curve for 0.1% wt. Alumina Nanofluid at 50 Psi

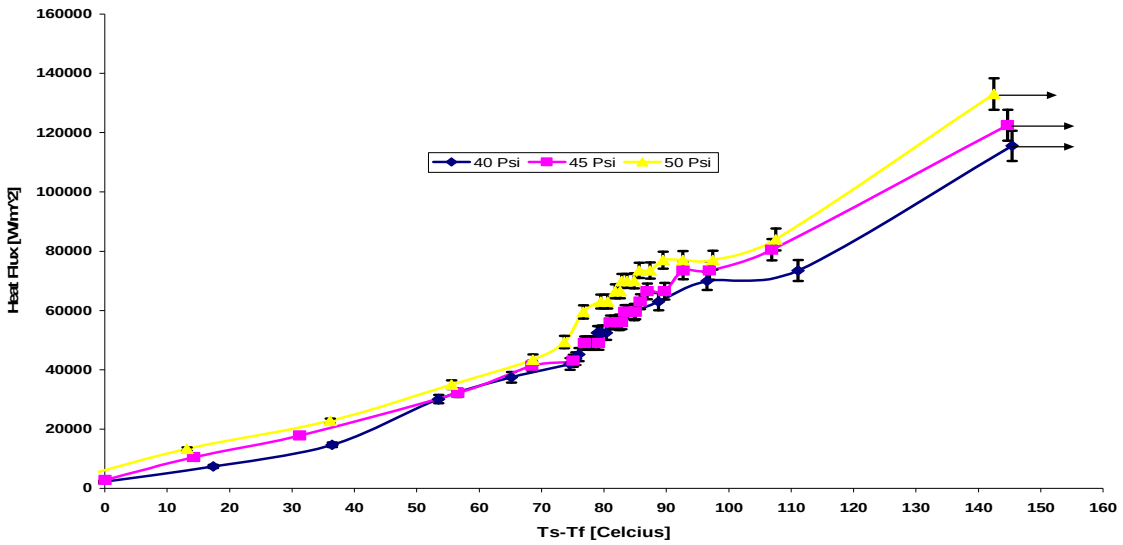

Figure 23: Spray Cooling Curve Comparison for 0.1% wt. Alumina Nanofluid at Different Pressures

Once again, increasing the pressure resulted in an increase in the heat flux at the spray surface. The CHF data collected and the corresponding temperature for each pressure is given below:

Table 8: Critical Heat Flux for 0.1% wt. Alumina Nanofluid

Pressure [Psi]	Critical Heat Flux [W/m^2]	Temperature [Celsius]
40	115,500	145.2
45	122,500	144.7
50	133,000	142.3

Increasing the pressure from 40 to 45 Psi results in an increase of 6.1% to the CHF and increasing the pressure from 45 to 50 Psi gives an 8.6% increase. The spray cooling experiments show the same results for water and alumina nanofluids, increasing the mass flow rate of droplets enhances heat transfer at the surface. The objective of the study was to investigate enhancements when compared to water at the same pressure. Therefore, the alumina nanofluid data was compared to water at the same pressure.

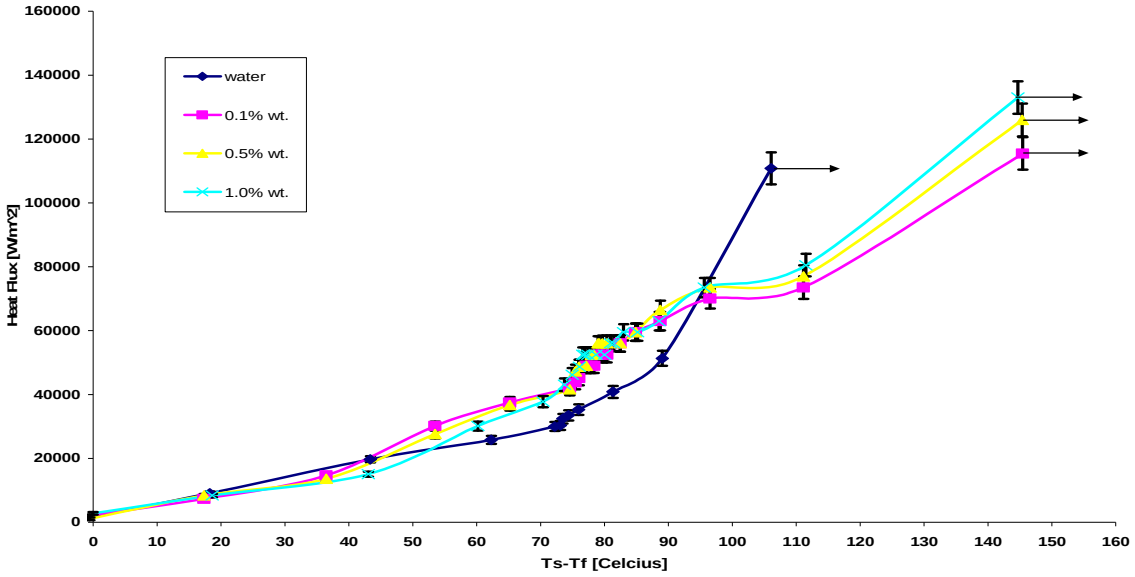

Figure 24: Spray Cooling Curve Comparison of Water vs. Nanofluids at 40 Psi

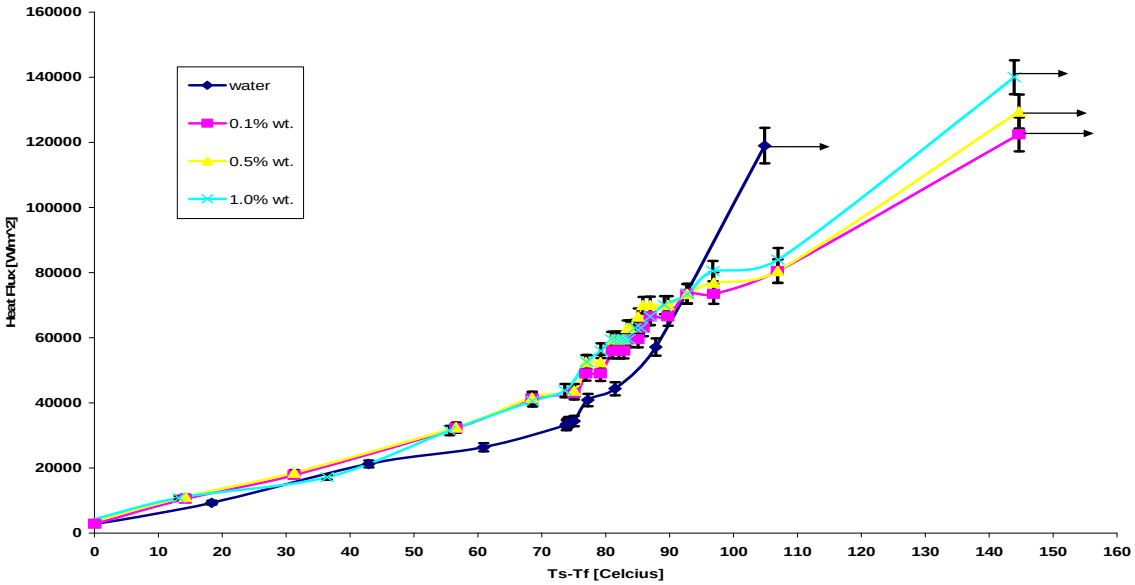

Figure 25: Spray Cooling Curve Comparison of Water vs. Nanofluids at 45 Psi

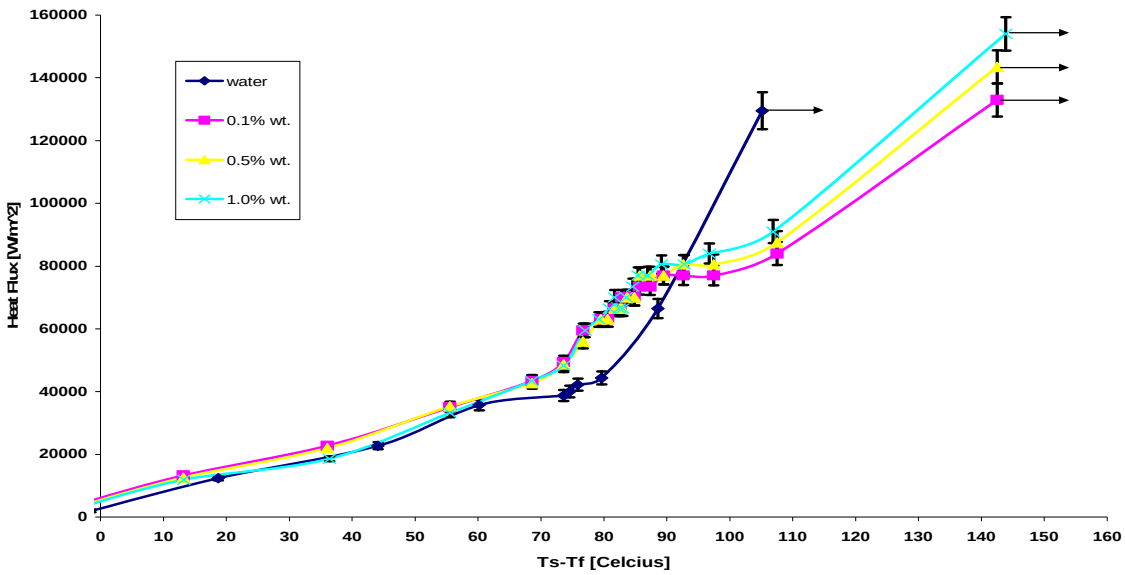

Figure 26: Spray Cooling Curve Comparison of Water vs. Nanofluids at 50 Psi

The data shows that the addition of alumina nanoparticles to water had a positive effect on single-phase and part of two-phase heat transfer during spray cooling experiments. The data also shows a shift to the right of the spray cooling curve, indicating a delay in two-phase heat transfer for all three pressures investigated. The heat transfer enhancement can be seen by an upward shift of the spray cooling curve when using alumina nanofluids. For example, at a pressure of 50 Psi and a temperature difference of approximately 79 ˚C, the heat flux at the spray surface for 1.0% wt. alumina nanofluid is calculated as 63,000 W/m^2 compared to only 44,333.3 W/m^2 with water. That result, shows a 42% increase in the heat flux removed from the heated surface. One possible explanation for the enhancement in heat transfer at the surface is the increase in wettability of the water by the addition of nanoparticles. Wetting is the ability of a liquid to remain in contact with a solid surface. Coursy *et al.* (2007) cited the increase in wettability as a possible mechanism in his pool boiling experiments. Since, the copper

spray surface was oriented horizontally the droplets traveled across the heated surface, by the force of gravity, removing heat. If the water's wettability increased with the addition of alumina nanoparticles, the droplets surface area in contact with the surface increased as they moved along the surface, therefore increasing heat transfer at the surface. Another mechanism for the increase in single-phase heat transfer is the time it takes for a droplet to travel the length of the heated surface. The increase in wettability will make the droplets attach to the surface longer increasing the ability for the droplet to remove heat. The data also shows that the mass concentrations of nanoparticles have little effect on the heat transfer enhancement during spray cooling. The nanofluids also showed enhancements to the CHF at all three pressures. The CHF enhancement was noticed to be effected by the mass concentrations of the nanofluids. At a mass concentration of 1.0% wt. the CHF had an average increase of 18.8%. An average increase of 11.1% and 3.3% was achieved with 0.5% wt. and 0.1% wt. mass concentrations respectively. The spray cooling experiments with nanofluids also showed a delay in two-phase heat transfer. The delay is characterized by a shift to the right of the spray cooling curve. One possible mechanism investigated for the increase in CHF and the delay in two-phase heat transfer was the surface roughness of the spray surface. The nanoparticles used in this investigation were a number of magnitudes smaller than the surface roughness of the spray surface. The nanoparticles are deposited to the surface by the vaporized water droplets. As a result, the nanoparticles become impinged in the surface crevices and change the characteristics of the surface. Once a layer of nanoparticles is deposited onto the surface, a new thermal resistance is introduced and the number of nucleation sites is reduced. The heat flux at the surface will have to be conducted through the deposited

alumina nanoparticles, which have a lower thermal conductivity than the copper surface, before being removed by the spray cooling process. A profilometer was used to measure the surface roughness of the spray surface before and after spray cooling with nanofluids and after the cleaning procedure had been performed.

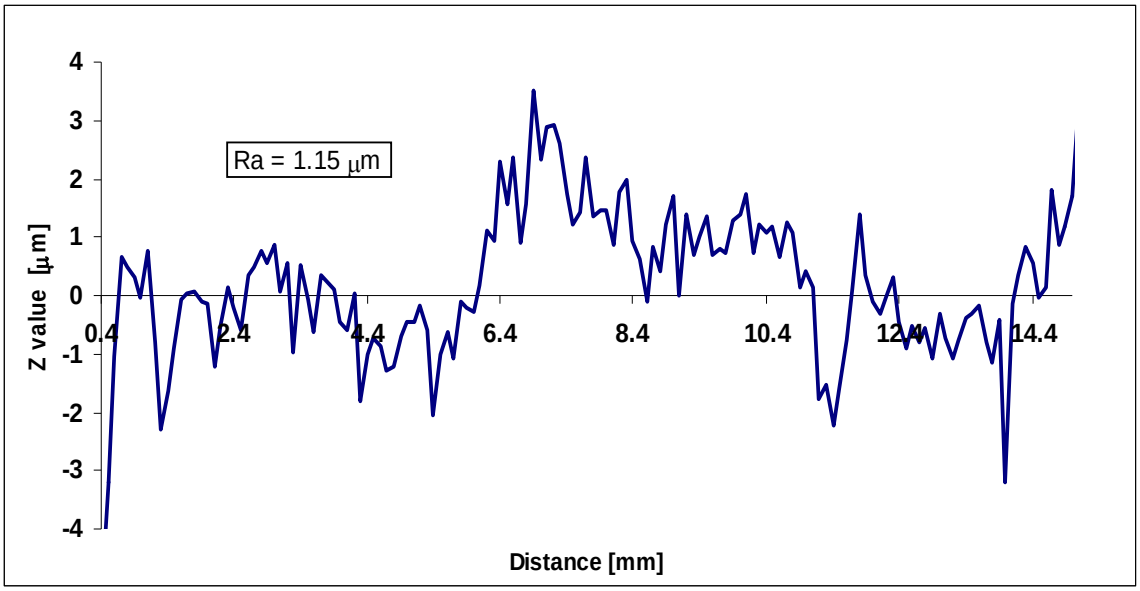

Figure 27: Surface Roughness before Spray Cooling

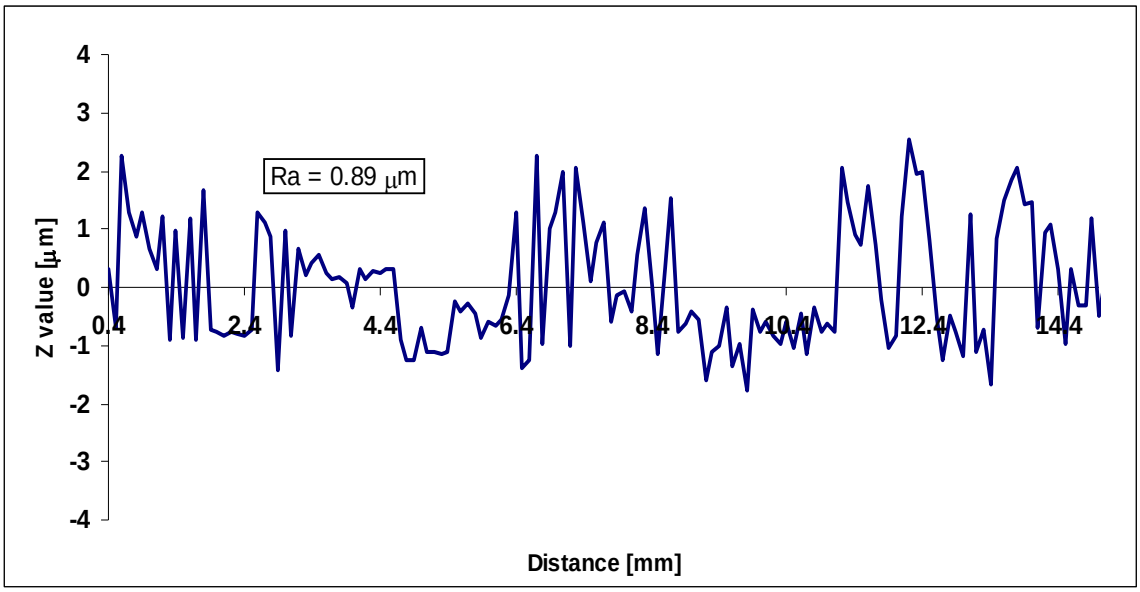

Figure 28: Surface Roughness after Spray Cooling with 0.5% wt. Alumina Nanofluid

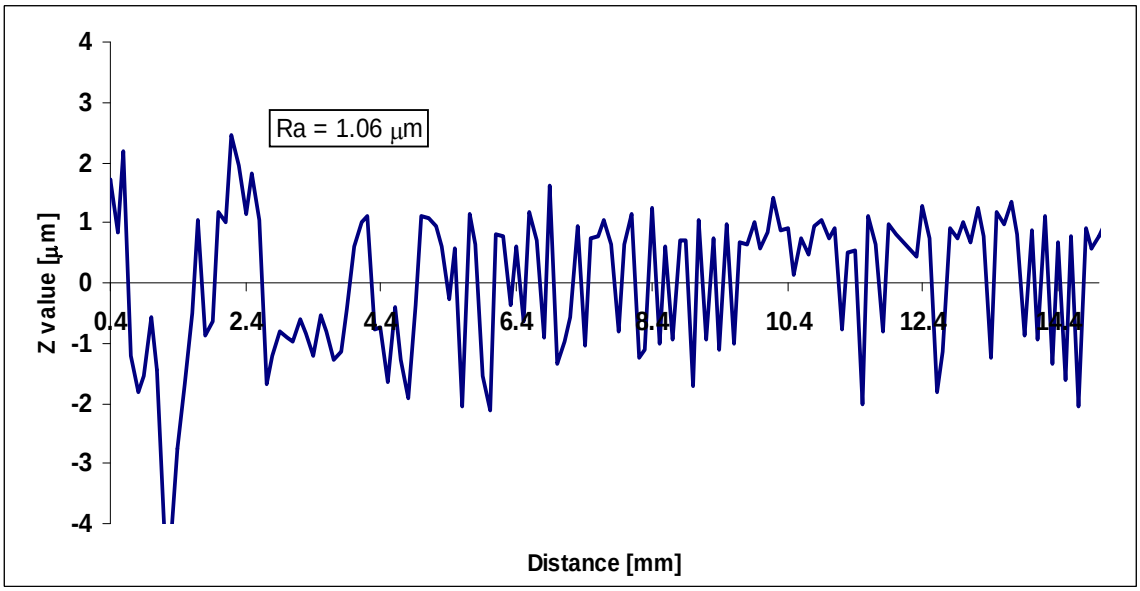

Figure 29: Surface Roughness after Cleaning Procedure

The results of the surface roughness measurements show the effects by the addition of alumina nanoparticles to water. The average roughness (Ra) value before spray cooling is found to be 1.15 μm. After spray cooling with a mass concentration of 0.5% wt. the surface roughness is measured again and found to have decreased to 0.89 μm. The

results of the surface roughness measurements indicate that the impinged alumina nanoparticles have made the copper surface smoother. To ensure the repeatability of the experiment, the surface roughness was measured after the cleaning procedure was performed. The cleaning procedure returned most of the roughness back to the surface and was found to be 1.06 μm. The impinged alumina nanoparticles on the copper spray surface have decreased the nucleation site density of the surface where the droplets change phase into vapor form. The reduction of vapor on the heated surface caused a delay in two-phase heat transfer. Two-phase heat transfer is desirable because it is a more effective way to remove heat when compared to single-phase heat transfer. Two-phase heat transfer utilizes the latent heat of evaporation of the working fluid to cause a phase change from liquid to vapor. This process is endothermic, which means that energy is absorbed by the droplets from the heated surface in going from liquid to vapor. Since a vapor blanket cannot form as easily once the surface has become fouled by the alumina nanoparticles, an increase in the CHF during spray cooling is found to occur. During pool boiling experiments CHF is characterized by a layer of vapor that forms at the heated surface preventing the working fluid from coming in contact with the surface, resulting in an increase in temperature. Similarly, during the spray cooling experiments, a vapor blanket formed over the heated copper surface which prevented the droplets from impinging the surface. The hot vapor blanket over the surface is not effective at conducting heat away from the surface, because of the low heat transfer coefficient of the vapor, which results in an increase in the temperature of the spray surface. The delay in two-phase heat transfer caused by the impingement of alumina nanoparticles allows for heat transfer to continue past the CHF point of water. The higher surface temperatures

experienced during the delay increased the heat flux at the surface and led to an increase of the CHF when alumina nanofluids where used as the working fluid. Higher CHF values resulted when using higher mass concentrations of alumina nanoparticles, though a further delay in CHF was not a function of mass concentration. Theoretically, the higher mass concentration alumina nanofluids deposit more nanoparticles onto the surface than the lower concentrations during the length of the experiment. This could have lead to less vapor and higher temperatures with higher mass concentrations.

Chapter 6 – Conclusion and Recommendations

6.1 Conclusion

The results of the investigation show that adding nanoparticles to the de-ionized water enhanced single-phase heat transfer as indicated by an increase in heat flux at the surface by as much as 42% when compared to water at the same temperature difference and pressure. One reason for this enhancement could be the change of the hydrodynamic characteristics of water. The addition of nanoparticles made the water more wettable and increased the wetting angle of the droplets. The droplets were able to remain in contact with the heated copper surface longer, increasing their effectiveness to remove heat. The horizontal position of the heated surface had an effect on the enhancement as well. With the horizontal orientation the droplets that impinged the surface at the top of the heated surface dragged across the surface by the force of gravity and heat was removed more effectively. The mass concentration of the nanoparticles seemed to have little to no effect on the single-phase heat transfer enhancement but did show effects with the increase in the CHF. All concentrations of nanoparticles resulted in a delay of two-phase heat transfer during the spray cooling investigation. The decrease in nucleation site density delayed the formation of vapor and increased the thermal resistance at the spray surface. The delay of two-phase heat transfer created higher surface temperatures which led to the increase in CHF. The higher mass concentration of 1.0% wt. resulted in an average

increase of 18.8% when compared to 0.5% wt. and 0.1% wt. with increases in CHF of 11.1% and 3.3% respectively

6.2 Recommendations

For future studies it will be important to investigate the results of altering the pH level of the nanofluid, since it has effects on the thermophysical properties of the nanofluid. The effects on the hydrodynamic properties of water by the addition of nanoparticles should also be considered. These properties could explain the enhancements to single-phase heat transfer and CHF. The orientation of the heated surface should be changed and its effects investigated. The copper block design could be improved to provide better efficiency of delivering the heat flux to the heated surface and not loosing much of it to the environment through the insulation. Much lower mass concentrations of nanoparticles, in the order of 0.001%, should be investigated to find an optimum concentration. To decrease the amount of nanofluids used during the investigation, a closed-looped system should be used.

References

Anoop, K. B., T. Sundararajan, and Sarit K. Das. "Effect of Particle Size on the Convective Heat Transfer in Nanofluid in the Developing Region." *International Journal of Heat and Mass Transfer* 52 (2009): 2189-95. Print.

Bang, Cheol In, and Soon Heung Chang. "Boiling Heat Transfer Performance and Phenomena of Al2O3–water Nano-Fluids from a Plain Surface in a Pool." *International Journal of Heat and Mass Transfer* 48 (2005): 2407-19. Web.

Choi, Stephen U. S., and J. A. Eastman. "Enhancing Thermal Conductivity of Fluids with Nanoparticles". *ASME International Mechanical Engineering Congress and Exposition.* November 12-17, 1995, San Francisco, CA. 1995. Print.

Chon, Chan Hee, Kenneth D. Kihm, and Shin Pyo Lee. "Empirical Correlation Finding the Role of Temperature and Particle Size for Nanofluid (Al[Sub 2]O[Sub 3]) Thermal Conductivity Enhancement." *Applied Physics Letters* 87 (2005): 153107. Print.

Coursey, Johnathan S., and Jungho Kim. "Nanofluid Boiling: The Effect of Surface Wettability." *International Journal of Heat and Fluid Flow* 29.6 (2008): 1577-85. Print.

Coursey, Johnathan S. "Enhancement of Spray Cooling Heat Transfer using Extended Surfaces and Nanofluids." Ph.D. University of Maryland, 2007. Print.

Das, Sarit K., Nandy Putra, and Wilfred Roetzel. "Pool Boiling Characteristics of Nano-Fluids." *International Journal of Heat and Mass Transfer* 46 (2003): 851-62. Print.

Duursma, Gail, Khellil Sefiane, and Aiden Kennedy. "Experimental Studies of Nanofluid Droplets in Spray Cooling." *Heat Transfer Engineering* 30.13 (2009): 1108-20. Print.

Hwang, Y. J., et al. "Investigation on Characteristics of Thermal Conductivity Enhancement of Nanofluids." *Current Applied Physics* 6 (2006): 1068-71. Print.

Incropera, Frank P., et al. "Impinging Jets." *Introduction to Heat Transfer.* 5th ed.Wiley, 2006. 402. Print.

Jang, Seok Pil, and Stephen U. S. Choi. "Role of Brownian Motion in the Enhanced Thermal Conductivity of Nanofluids." *Applied Physics Letters* 84 (2004): 21-4. Print.

Liu, Zhen-Hua, and Yu-Hao Qui. "Boiling Heat Transfer Characteristics of Nanofluids Jet Impingement on a Plate Surface." *International Journal of Heat and Mass Transfer* 43 (2007): 699-706. Print.

Murshed, S. M. S., K. C. Leong, and C. Yang. "Enhanced Thermal Conductivity of TiO2—water Based Nanofluids." *International Journal of Thermal Sciences* 44.4 (2005): 367-73. Print.

Nguyen, Cong Tam, et al. "An Experimental Study of a Confined and Submerged Impinging Jet Heat Transfer using Al2O3-Water Nanofluid." *International Journal of Thermal Sciences* 48.2 (2009): 401-11. Print.

Sefiane, K., and R. Bennacer. "Nanofluids Droplets Evaporation Kinetics and Wetting Dynamics on Rough Heated Substrates." *Advances in Colloid and Interface Science* 147 (2009): 263-71. Print.

Shen, Jian. "Hydrodynamics of Droplet Impingement on Heated Surfaces : Effects of Nanofluid and Nano-Structured Surface." Ph.D. Oregon State University, 2009. Web. 10/12/2009.

Trisaksri, Visinee, and Somchai Wongwises. "Nucleate Pool Boiling Heat Transfer of TiO2-R141b Nanofluids." *International Journal of Heat and Mass Transfer* 52 (2009): 1582-8. Print.

Vassallo, Peter, Ranganathan Kumar, and Stephen D'Amico. "Pool Boiling Heat Transfer Experiments in silica–water Nano-Fluids." *International Journal of Heat and Mass Transfer* 47.2 (2004): 407-11. Print.

Wen, Dongsheng. "Mechanisms of Thermal Nanofluids on Enhanced Critical Heat Flux (CHF)." *International Journal of Heat and Mass Transfer* 51.19-20 (2008): 4958-65. Print.

Xie, Huaqin, et al. "Thermal Conductivity Enhancement of Suspensions Containing Nanosized Alumina Particles." *Journal of Applied Physics* 91.7 (2002): 4568-72. Print.

Xuan, Yimin, and Qiang Li. "Heat Transfer Enhancement of Nanofluids." *International Journal of Heat and Fluid Flow* 21.1 (2000): 58-64. Print.

You, S. M., J. H. Kim, and K. H. Kim. "Effect of Nanoparticles on Critical Heat Flux of Water in Pool Boiling Heat Transfer." *Applied Physics Letters* 83.16 (2003): 3374-6. Print.

Zhang, Xing, and Hua Gu. "Effective Thermal Conductivity and Thermal Diffusivity of Nanofluids Containing Spherical and Cylindrical Nanoparticles." *Journal of Applied Physics* 100.4 (2006): 044325. Print.

Zhou, D. W. "Heat Transfer Enhancement of Copper Nanofluid with Acoustic Cavitation." *International Journal of Heat and Mass Transfer* 47.14-16 (2004): 3109-17. Print.

Zhu, Dongsheng, et al. "Dispersion Behavior and Thermal Conductivity Characteristics of Al2O3–H2O Nanofluids." *Current Applied Physics* 9.1 (2009): 131-9. Print.